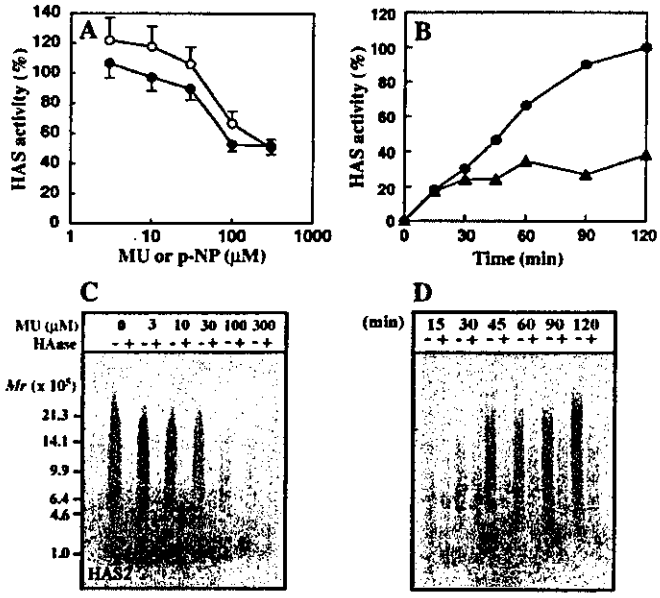

FIG. 2. **Effects of MU or *p*NP on HAS activity and size distribution of synthesized HA.** *A*, membrane-rich fraction from 3Y1-HAS2 cells was incubated with various concentrations of MU (*closed circles*) or *p*NP (*open circles*), and then HAS activity was calculated as a percentage relative to that of the nontreated sample. *B*, HAS activities were measured at various periods after the treatment of 3Y1-HAS2 transfectants without (*closed circles*) or with 300 μM MU (*closed triangles*). *C*, the same reaction supernatants were digested with (+) or without (−) 10 turbidity reducing units of *Streptomyces* hyaluronidase, and the size distributions of HA were then analyzed by 0.5% agarose gel electrophoresis. Radiolabeled HA was detected by autoradiography. Standard HA samples with known molecular size were used to determine the size distributions of newly synthesized HA. *D*, the time-dependent effect of MU on the chain elongation was assessed as above. *Plus* and *minus* indicate samples treated with or without 300 μM MU, respectively.

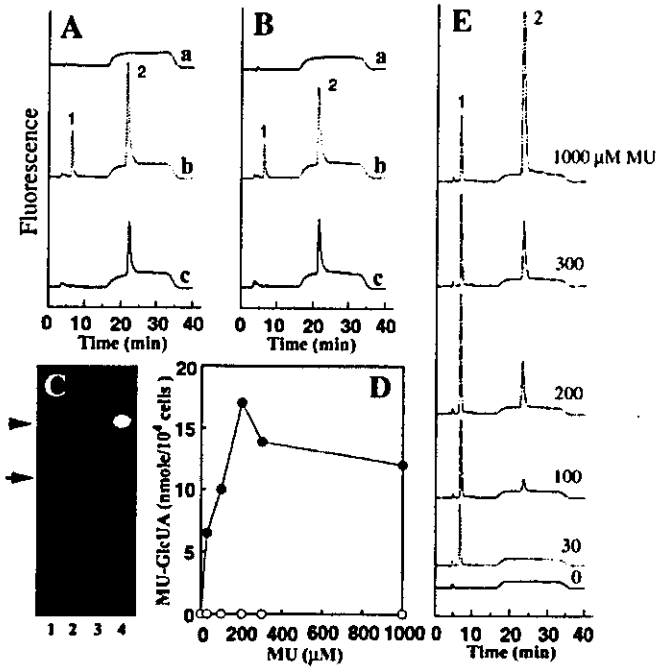

FIG. 3. **HPLC and TLC analyses of MU derivatives found in the culture conditioned medium.** 3Y1-HAS2 (*A*) and 3Y1-Mock (*B*) cells were incubated without (*a*) or with 1000 μM MU (*b* and *c*) for 24 h. The conditioned medium was analyzed before (*a* and *b*) and after digestion (*c*) with 1 unit of β-glucuronidase by HPLC on TSK gel ODS 120-T. *Peaks 1* and *2* corresponded to MU-GlcUA and MU used as authentic standards, respectively. *C*, peak 1 in the HPLC, with a retention time coinciding with that of an authentic MU-GlcUA standard, was collected and analyzed by TLC. *Lane 1*, standard MU-GlcUA; *lane 2*, peak 1 from 3Y1-HAS2 cells; *lane 3*, peak 1 from 3Y1-Mock cells; *lane 4*, standard MU. *D*, 3Y1-HAS2 cells were treated with various concentrations of MU for 24 h, and the production amounts of peak 1 in the conditioned medium (*closed circle*) and in the cell lysate (*open circle*) were expressed per viable cell number. *E*, HPLC profiles of MU derivatives from 3Y1-HAS2 cells treated with various concentrations of MU for 24 h.

compounds in mammalian cells, particularly in the liver (38). Because HAS possesses a glycosyltransferase activity for UDP-GlcUA within its polypeptide (17), we initially hypothesized that the enzyme is able to transfer GlcUA to MU from UDP-GlcUA, and the glucuronidation of MU competitively inhibits chain elongation of HA. We therefore tested the effect of *p*NP, another acceptor for UGTs (39), on HAS activity. As shown in Fig. 2*A*, HAS activity was indeed inhibited by *p*NP.

Production of MU-GlcUA in the Culture Medium and in the Reaction Supernatant of the Cell-free HA Synthesis—The effects of both MU and *p*NP prompted us to investigate whether the glucuronidation of these compounds is involved in the inhibition of HAS activity. The production of MU-GlcUA was analyzed by HPLC by using conditioned medium from 3Y1-HAS2 and 3Y1-Mock cells which were cultured for 24 h in the presence of various concentrations of MU. In the presence of MU, two major peaks appeared with a retention time of ~7 and 22 min (Fig. 3, *A* and *B*). The peak 2 at 22 min corresponded to that of the MU standard, whereas the peak 1 at 7 min was identified as MU-GlcUA because this coincided with that of an authentic standard sample and was sensitive to treatment with β-glucuronidase. Interestingly, a similar level of MU glucuronidation was observed in the control 3Y1-Mock cells (Fig. 3*B*) which express low levels of endogenous HAS2 and HAS3. This suggests that glucuronidation was mediated by the endogenous UGT activity expressed in the 3Y1 host cells. The MU derivative in peak 1, collected from the HPLC fraction, migrated on TLC at the same position as authentic standard MU-GlcUA (Fig. 3*C*). To estimate the molecular weight of the MU derivative, the peak 1 observed on HPLC was collected and subjected to mass spectrometry. The negative ion mass spectrum of the peak 1 from 3Y1-HAS2, shown in Fig. 4, had a $[M - H]^-$ ion peak at m/z 351. Therefore, the molecular weight of the MU derivative in peak 1 was determined to be 352, which was consistent with the calculated mass for MU-GlcUA ($C_{16}H_{16}O_9$; M_r = 352). The molecular ion at m/z 351 was also determined when the peak 1 from 3Y1-mock was used. The combined results of HPLC, TLC, and mass spectrometry confirmed that the MU derivative in peak 1 is MU-GlcUA (chemical structure is shown in Fig. 4). When 3Y1-HAS2 cells were cultured with various concentrations of MU, maximal production of MU-GlcUA was observed at 200 μM of MU (Fig. 3, *D* and *E*) both in the culture-conditioned medium and in the cell lysate. Most MU-GlcUA was secreted into the culture medium (Fig. 3*D*). The production of MU-GlcUA in the cell lysate was 60 fmol/10^4 cells at 200 μM of MU, which was much less than that in the culture conditioned medium, 17.0 nmol/10^4 cells. The secretion may be mediated by ATP-binding cassette transporters of the multidrug resistance protein family as demonstrated in the other cell systems (40). It was difficult to estimate the ratio of the UDP-GlcUA consumed for production of MU-GlcUA to total intracellular UDP-GlcUA. It seems, however, reasonable to assume that the amount of UDP-GlcUA, which had been consumed to produce MU-GlcUA, is equal to (or more than) the amount of the produced MU-GlcUA. Total amounts of secreted and intracellular MU-GlcUA suggested that 22.8 and 9.4% of loaded MU was converted to MU-GlcUA at the concentrations of 30 and 300 μM, respectively.

Transglycosylation of GlcUA to MU or *p*NP was confirmed by TLC analysis of the cell-free reaction mixture. When UDP-

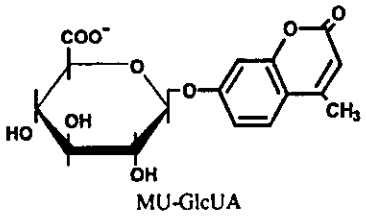

MU-GlcUA

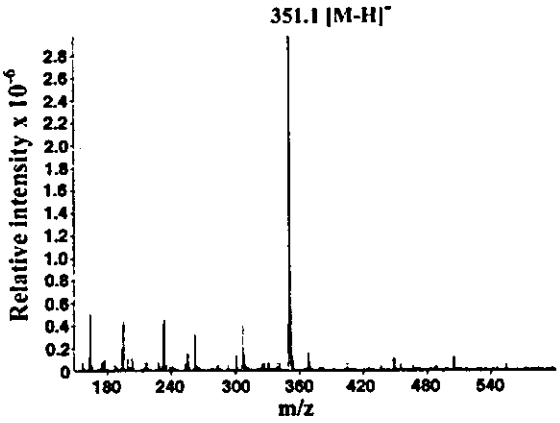

FIG. 4. **Chemical structure of MU-GlcUA and mass spectrum of MU derivative.** Peak 1 from 3Y1-HAS2, eluted at the same position of authentic standard MU-GlcUA in the HPLC (Fig. 3), was collected and analyzed by mass spectrometry. The conditions were described under "Experimental Procedures."

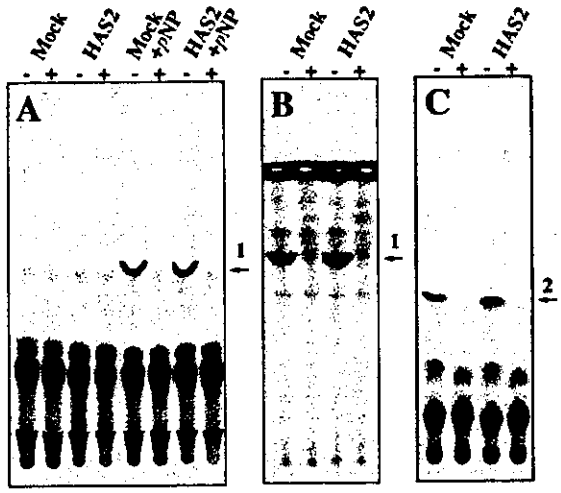

FIG. 5. **TLC analysis of *p*NP- or MU-GlcUA produced in the supernatant of the cell-free HA synthesis.** The membrane-rich fractions from 3Y1-Mock or 3Y1-HAS2 cells were incubated in the presence of UDP-[^{14}C]GlcUA and *p*NP (*A*), or UDP-GlcUA and [^{14}C]*p*NP (*B*), or UDP-[^{14}C]GlcUA and MU (*C*), and the reaction supernatants were analyzed by TLC on a Silica 60 plate as described under "Experimental Procedures." *Arrow 1* and *2* show the positions corresponding to those of the standard *p*NP- or MU-GlcUA, respectively. *Minus* and *plus* show samples before and after treatment with 2 units of β-glucuronidase.

[^{14}C]GlcUA was used to monitor the glucuronidation, radiolabeled spots corresponding to authentic MU-GlcUA or *p*NP-GlcUA used as standards were produced by endogenous UGTs in the presence of MU or *p*NP, respectively (Fig. 5, *A* and *C*). When UDP-GlcUA and [^{14}C]*p*NP were added to the cell-free HA synthesis, radiolabeled spots corresponding to *p*NP-GlcUA were also detected on TLC (Fig. 5*B*). The radiolabeled spots disappeared after treatment with β-glucuronidase, showing that GlcUA was transferred from UDP-GlcUA to MU or *p*NP in the cell-free HA synthesis. Our experiments suggest that HAS does not mediate the glucuronidation of MU or *p*NP, because MU-GlcUA and *p*NP-GlcUA were detected using both 3Y1-HAS2 and 3Y1-Mock cells.

Effect of MU-GlcUA on the HAS Activity—MU and *p*NP derivatives of xylosides, MU-Xyl and *p*NP-Xyl, have been shown to act as artificial primers for the initiation of glycosaminoglycan synthesis in cultured mammalian cells (41, 42). These derivatives behave as native primers. We then considered the possibility that MU-GlcUA and *p*NP-GlcUA might affect the initial step in HA elongation. To examine this possibility, MU-GlcUA or *p*NP-GlcUA was added to the cell-free HA synthesis. As expected, HAS activity was inhibited by MU-GlcUA or *p*NP-GlcUA in a dose-dependent manner (Fig. 6, *A* and *B*). However, the inhibitory activity of these compounds was far less than that of aglycon, MU, and *p*NP, suggesting that they do not directly inhibit HA synthesis. Surprisingly, similar results were also obtained using other sugar derivatives of MU or *p*NP, *i.e.* MU-GlcNAc, MU-Glc, *p*NP-GlcNAc, and *p*NP-Glc. Indeed when any of the *p*NP sugar derivatives were incubated with UDP-[^{14}C]GlcUA in the cell-free HA system, the *de novo* production of radiolabeled *p*NP-GlcUA was detected by TLC (Fig. 6*C*). However, radiolabeled *p*NP-GlcUA was absent when the *p*NP sugar derivatives were incubated without the membrane fraction (data not shown). The *de novo* production of radiolabeled *p*NP-GlcUA could be due to the liberation of *p*NP or MU from its respective sugar derivative and the transfer of GlcUA to the free aglycon from UDP-GlcUA by the endogenous UGT activity. Therefore, the inhibition of HAS activity may be dependent on the repeated glucuronidation of the free aglycon liberated from the sugar derivatives.

UGTs Enhanced the Inhibition of HAS Activity by MU—Although our results suggested that MU-GlcUA did not directly inhibit HAS activity, the production of MU-GlcUA by the endogenous UGTs seemed to be important for inhibition. We therefore investigated whether the inhibitory effect of MU and *p*NP was related to glucuronidation. To test this hypothesis, we examined the effect of recombinant UGT proteins on the inhibition by MU or *p*NP. Increased glucuronidation of *p*NP was observed by TLC when a recombinant UGT1A6 protein was added to the reaction mixture of cell-free HA synthesis (Fig. 7*B*). Under the same conditions used in the TLC analysis, the recombinant UGT significantly enhanced the inhibitory effect of *p*NP on HA synthesis (Fig. 7*A*). In contrast, UGT did not affect the HAS activity in the absence of *p*NP regardless of whether it was active or not. Almost the same degree of inhibition was observed by adding UGT1A7, which is one of the isoforms, in the presence of *p*NP or MU (Fig. 7*C*). These results suggested that the inhibition of HAS activity was directly related to extent of glucuronidation mediated by UGT.

The link between the inhibition of HAS and glucuronidation was further confirmed using the transfectants overexpressing a human UGT1A6 isoform (Fig. 8). The UGT1A6 and/or HAS2 expression plasmids were transiently transfected into COS cells, and the HAS activity was then measured in the presence or absence of 100 μM MU. COS cells do not express any UGT activity, as only a trace amount of MU-GlcUA was detected by TLC in the case of the membrane-rich fraction from the Mock or HAS2 transfectants (Fig. 8*B*). However, a large amount of MU-GlcUA was detected when UGT1A6 was expressed in the COS cells (Fig. 8*B*). The system is therefore suitable for investigating the effects of MU glucuronidation on the HAS activity. When COS cells co-transfected with both UGT1A6 and HAS2 cDNA were treated with MU, HAS activity was only 30% that of the untreated control value (Fig. 8*A*). However, for the membrane-rich fraction from transfectants expressing HAS2 alone, only a slight decrease in HAS activity was observed in the

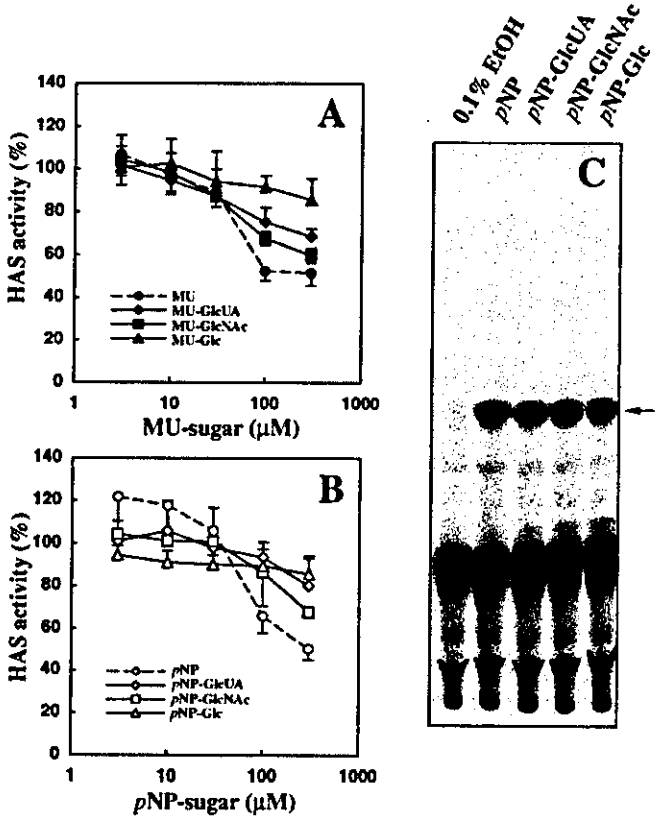

FIG. 6. **Effects of MU- and *p*NP-sugars on HAS activity.** The effects of various sugar derivatives of MU (*A*) or *p*NP (*B*) were assessed by cell-free HA synthesis. Various concentrations of MU (*closed circles*), MU-GlcUA (*closed diamonds*), MU-GlcNAc (*closed squares*), MU-Glc (*closed triangles*), *p*NP (*open circles*), *p*NP GlcUA (*open diamonds*), *p*NP-GlcNAc (*open squares*), and *p*NP-Glc (*open triangles*) were added in the membrane-rich fractions prepared from HAS2 transfectants, and then the HAS activities were calculated as percentages relative to that of the nontreated sample. Data represent average of three independent experiments ± S.D. *C*, membrane-rich fractions from 3Y1-HAS2 cells were incubated with 100 μM *p*NP-sugars and UDP-[^{14}C] GlcUA, and the production of *p*NP-GlcUA was analyzed on TLC. Radiolabeled spots corresponding *p*NP-GlcUA (*arrow*) were detected by autoradiography.

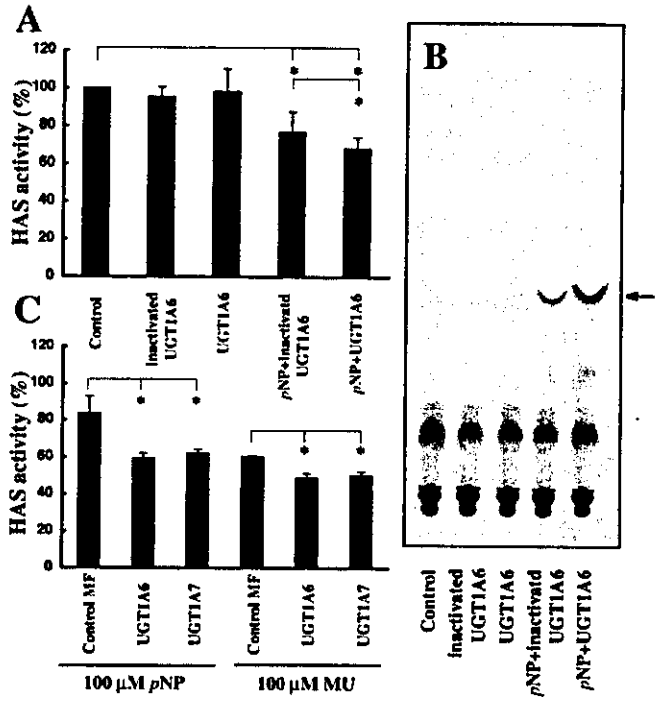

FIG. 7. **Enhanced inhibition of HAS activity by recombinant UGT proteins.** *A*, partially purified recombinant human UGT1A6 was added together with 100 μM *p*NP in the cell-free HA synthesis, and then the HAS activities were calculated as percentages relative to the nontreated sample. Inactivated UGT1A6 was obtained by boiling the active enzyme. Data represent average of three independent experiments ± S.D. *, $p < 0.05$. *B*, membrane fractions from 3Y1-HAS2 cells were incubated with 100 μM *p*NP and UDP-[^{14}C]GlcUA, and the production of *p*NP-GlcUA was analyzed on TLC. Radiolabeled spots corresponding *p*NP-GlcUA (*arrow*) was detected by autoradiography. *C*, partially purified UGT1A6 or UGT1A7 was added together with 100 μM *p*NP or MU in the cell-free HA synthesis system, and then the HAS activities were calculated as percentages relative to the nontreated sample. Membrane fractions prepared from insect cells infected with baculovirus vector alone were used as a control membrane fractions. Data represent average of three independent experiments ± S.D. *, $p < 0.05$.

presence of MU (Fig. 8*A*). HA production into the conditioned medium was also measured when these transfectants were cultured with or without MU. The results were similar to those obtained using the cell-free system (Fig. 8*C*). Taken together, these results suggest that the inhibition of HA synthesis by MU or *p*NP is caused by the UGT-dependent glucuronidation of these compounds.

Effect of UDP-GlcUA on the Inhibition of HAS Activity by MU—The inhibition of HA synthesis may be caused by a depletion in the pool of UDP-GlcUA due to UGT-mediated MU glucuronidation. If this hypothesis is correct, we would expect HAS activity to recover after addition of an excess amount of UDP-GlcUA to the cell-free HA synthesis, even in the presence of MU. Indeed, we did observe the recovery of HAS activity following addition of UDP-GlcUA in a dose-dependent manner (Fig. 9*A*). UDP-GlcUA was then added to the reaction mixture 1 h after the initiation of HA synthesis. The HAS activity inhibited by the MU treatment was partially rescued when the UDP-GlcUA concentration increased (Fig. 9*B*). We also determined whether HAS inhibition was enhanced by pretreatment of the membrane fraction with MU prior to the initiation of the HA synthesis. If the kinetic lag shown in Fig. 2*B* reflects the duration for the depletion of UDP-GlcUA in the reaction mixture or formation of MU derivative inhibitor, then the preincubation would inhibit HAS activity more completely. However, time-dependent changes in the HAS activity revealed that the kinetic lag still remained, and the effect was minimal at an early incubation time (Fig. 10). Furthermore, the pretreatment of membranes with MU-GlcUA had a lesser effect on HAS activity than that of MU (Fig. 10), suggesting that the HAS activity is not inhibited irreversibly by MU-GlcUA. This was also confirmed by the experiment where HAS activity was measured under the MU-GlcUA-free conditions using membrane fractions pretreated with 300 μM MU-GlcUA (data not shown). A similar result was also obtained when the membrane fractions were pretreated with 300 μM MU (data not shown). Taken together, the results suggest that the glucuronidation event followed by the subsequent reduction of UDP-GlcUA concentration affects the HAS activity at the late stage of HA elongation.

DISCUSSION

In this study we present a novel mechanism for the inhibition of HA synthesis involving the UGT-dependent glucuronidation of MU. Although MU has been widely used as an inhibitor of HA synthesis (10, 25, 26), the exact inhibitory mechanism is not clear, especially in mammalian cells. A major problem in the elucidation of this inhibitory mechanism has been the complexity of the HA synthetic system that is regulated by three related mammalian HAS isoforms, HAS1, HAS2, and HAS3 (17). To reduce this complexity we initially established three rat 3Y1 cell lines, each expressing a distinct HAS isoform, to test whether MU inhibited HA production and ma-

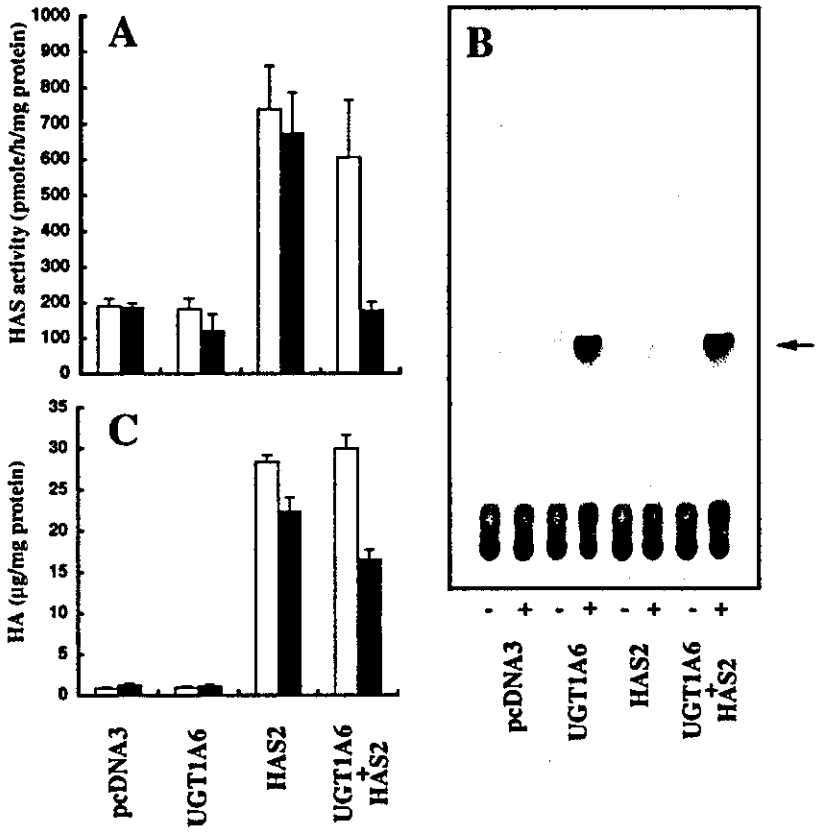

FIG. 8. **Overexpression of human UGT1A6 enhanced the inhibition of HAS activity and HA synthesis by MU.** *A*, membrane-rich fractions from COS transfectants expressing UGT1A6 and/or HAS2 were incubated with (*solid bars*) or without (*open bars*) 100 μM MU, and the HAS activities were then calculated as percentages relative to the control. *B*, membrane-rich fractions from COS transfectants were incubated without or with 100 μM MU and UDP-[^{14}C]GlcUA, and the production of MU-GlcUA was analyzed on TLC. Radiolabeled spots corresponding to MU-GlcUA (*arrow*) were detected by autoradiography. *Plus* and *minus* indicate samples in the presence or absence of MU, respectively. *C*, the HA contents in the conditioned medium of COS transfectants expressing UGT1A6 and/or HAS2 were measured by ELISA-like assay 24 h after the treatment with (*solid bars*) or without (*open bars*) 300 μM MU. Data represent average of three independent experiments ± S.D.

trix formation in a similar way to that observed for human skin fibroblasts (23, 24). When the cells were cultured in the presence of MU, a decrease in both HA production and matrix formation was observed in all three transfectants, and in particular the HAS2 transfectant (data not shown). Therefore, we adopted HAS2 expressing cells to further elucidate the inhibition mechanism of MU in this study.

We had observed previously growth suppression of human skin fibroblasts when treated with a high concentration of MU. HA synthesis is known to be down-regulated in growth-arrested cells (43). Our recent study (44) also suggested that HAS gene expression is regulated via signaling cascades linked to cell proliferation. Therefore, we investigated whether the antiproliferative effect of MU lowers the expression of HAS and subsequently HA synthesis. At low and moderate concentrations of MU, however, we could not detect any significant change in the transcriptional levels of endogenous HAS genes in the rat 3Y1 transfectants, despite the significant decrease in HA synthesis. The fact that MU inhibited HA synthesis, even in the transfectants in which HAS expression is driven by an exogenous promoter, suggested the post-transcriptional inhibition of HA synthesis. However, we could not rule out the possibility that MU down-regulated the promoter activity of the endogenous HAS genes because they were moderately suppressed at high concentrations of MU.

To avoid the influence of growth suppression, we examined the effect of MU on HAS activity in a cell-free system. The HAS activity in the crude membrane fraction from the HAS2 transfectants was inhibited by MU treatment. The result is consistent with the idea that MU inhibits HA synthesis post-transcriptionally and in a growth-independent fashion. Interestingly, a similar result was obtained when *p*NP was tested for the ability to inhibit HAS activity in the cell-free HA synthesis. This led us to examine whether these two compounds, known to be good substrates for UGT, can act as acceptors for glucuronyltransferase of HAS. A substantial amount of glucuronidation of MU was observed in the conditioned medium and in the supernatant of the cell-free HA synthesis. Intriguingly, a considerable amount of glucuronidation was also observed in the control cells expressing very little HAS, suggesting that MU was glucuronidated by an endogenous UGT other than HAS. Monosaccharide derivatives of MU and *p*NP have been shown to act as artificial primers for the initiation of glycosaminoglycan biosynthesis in cultured mammalian cells (41, 42). In plants, the lipid-sugar conjugate has been shown to act as a primer in the synthesis of cellulose (45). We considered the possibility that MU-GlcUA may act as an artificial initiation primer for HA synthesis thereby decreasing the efficiency of HA polymerization, the primary role of HAS. However, this hypothesis seemed unlikely because the inhibition rate of MU-GlcUA was less than that of MU. Moreover, no elongation products of MU-GlcUA were detected in the conditioned medium or in the supernatant of the cell-free HA synthesis (data not shown). Alternatively, previous studies (23, 46) have shown that MU and *p*NP derivatives of xylosides, MU-Xyl and *p*NP-Xyl, significantly inhibited the biosynthesis of HA as well as sulfated glycosaminoglycans. As for the mechanism, it was suggested that free *p*NP, which is generated by the enzymatic hydrolysis of *p*NP-Xyl, mediated the inhibitory effect (47). In the current study, we also detected a significant liberation of *p*NP from its sugar derivatives. These results together with our finding that glucuronidation of the free aglycons occurred in parallel with the increased inhibition rate of HA synthesis support the importance of the glucuronidation in the inhibition.

Elevating the level of MU-GlcUA, by addition of exogenous recombinant UGT, promoted the inhibition of HA synthesis in the cell-free system. Furthermore, when COS cells overexpressing UGT and HAS2 were treated with MU, the inhibitory effects were enhanced both in terms of HAS activity and HA production. Excess glucuronidation of MU by UGT could deplete the pool of UDP-GlcUA, which is a common substrate for HAS and UGT. As shown in Fig. 9*A*, the inhibition of HA

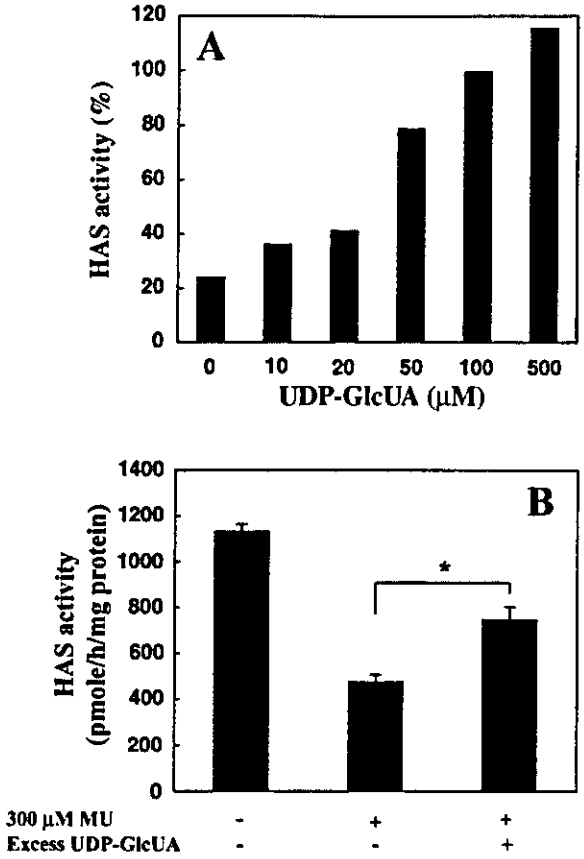

FIG. 9. **Excess amount of UDP-GlcUA diminished the effect of MU on HAS activity.** *A*, various concentrations of UDP-GlcUA were added together with 100 μM MU in the membrane-rich fractions from COS transfectants co-expressing UGT1A6 and HAS2, and the HAS activities were then calculated as percentages relative to that of the nontreated sample. The inhibitory effect of MU was diminished to the control level by an excess amount of UDP-GlcUA. *B*, the membrane-rich fractions from COS transfectants co-expressing UGT1A6 and HAS2 were preincubated for 1 h with (+) or without (−) 300 μM MU in the reaction buffer as described under "Experimental Procedures." Additional UDP-GlcUA was then supplied at the concentration of 0.1 mM to the reaction mixture and further incubated at 37 °C for 1 h. The inhibition of HAS after treatment with MU was partially rescued at the increased concentrations of UDP-GlcUA. Data represent average of three independent experiments ± S.D. *, $p < 0.05$.

synthesis was reduced to the control level when an excess of UDP-GlcUA was added to the *in vitro* reaction mixture. Thus, it is conceivable that the cellular concentration of UDP-GlcUA could be an important factor in the inhibitory action of MU. To clarify the mode of action, we determined whether the HAS inhibition was enhanced by pretreatment of the membrane fraction with MU or MU-GlcUA prior to initiating HA synthesis. Time-dependent changes in HAS activity demonstrated that pretreatment with MU exerted little effect on the inhibition of HA synthesis at the initiation step (Fig. 10). However, the inhibition of HAS activity after MU treatment was partially rescued by increasing the UDP-GlcUA concentration at the later time points (Fig. 9*B*). Taken together, the results suggest that the glucuronidation event followed by the subsequent reduction of UDP-GlcUA concentration predominantly affects the chain elongation after the lag period of HAS inhibition. Consistent with this idea, the chain elongation of HA was reduced by MU after the lag period as shown in Fig. 2. This could be rationalized by assuming that the K_m value for UDP-GlcUA of HAS enzymes is altered in a manner depending on the chain length of synthesizing HA.

The glucuronidation event may affect HAS activity to a greater extent in the cells expressing elevated levels of UGTs.

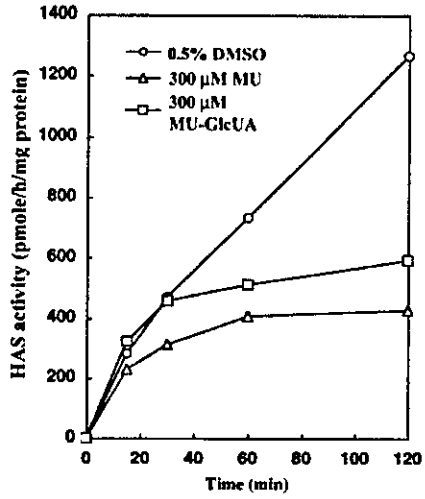

FIG. 10. **Pretreatment of the membrane fractions with MU or MU-GlcUA.** The membrane fractions isolated from 3Y1-HAS2 transfectants were preincubated for 1 h with 0.1 mM UDP-GlcUA in the presence of 300 μM MU or MU-GlcUA. The HA synthesis was then initiated by addition of a saturated concentration of UDP-GlcNAc, and time-dependent changes in the HAS activity were monitored by the incorporation of radioactivity into the HA fraction. A slight inhibition of HAS activity was observed at 15 min and became more apparent thereafter. The effect of MU-GlcUA was less than that of MU itself. Data represent average of two independent experiments.

Indeed, MU significantly lowered HAS activity in rat 3Y1 cells expressing endogenous UGT, in contrast to COS cells that do not express any UGT. Altering the cellular level of UDP-GlcUA would be expected to mirror these observations. Depletion of UDP-GlcUA in the cellular pools may affect the biosynthesis of other GlcUA-containing glycosaminoglycans such as heparan sulfate and chondroitin sulfate. Previous studies, however, indicated that the action of MU had no affect on glycosaminoglycan biosynthesis in human skin fibroblasts (23, 24). We considered several possible explanations related to the selective inhibition of the synthesis by MU. MU may specifically target HAS due to its cellular localization, which is different from other glycosyltransferases, exostosin (EXT) family (48, 49) and chondroitin synthases (50–52) involved in the biosynthesis of heparan sulfate and chondroitin sulfate, respectively. All the glycosaminoglycans, with the single exception of HA, are synthesized at the intracellular Golgi network. HA is synthesized on the inner side of the plasma membrane by a membrane-associated HAS (17). The cell-free HA synthesis revealed that UGT activity is present in the membrane preparations. This is consistent with previous observations (53) in which most UGTs are present in the endoplasmic reticulum and nuclear membrane. Glucuronidation of MU may result in a differential reduction in the local concentration of UDP-GlcUA near the plasma membrane and in the Golgi and endoplasmic reticulum. Alternatively, this observation could be rationalized by assuming that the K_m value for UDP-GlcUA of these enzymes varies markedly. In previous work, however, the K_m values for UDP-GlcUA were similar among recombinant HAS2 (32), chondroitin synthases (51, 52), and UGT1A6 (54). Another explanation for the selective inhibition would be the preferential effects of MU on the chain elongation of a large molecular mass of HA (over 1×10^6 Da) as shown in Fig. 2.

One might expect a common inhibition mechanism for MU in both the mammalian cells and *Streptococcus*, because they synthesize HA with exactly the same structure by using homologous enzymes (17). A possibility of the post-transcriptional inhibitory mechanism was also speculated from the results in group C *Streptococcus* that MU did not affect the expression level of HAS (28). On the other hand, we speculated that MU

inhibits HA synthesis of group C *Streptococcus* in a cardiolipin-dependent fashion without significant change in HAS activity in the cell-free HA system. The discrepancy between this result and the observations reported in this paper may be due to a different level of MU-GlcUA in the *Streptococcus*. Indeed, the production of MU-GlcUA was not detected in either the conditioned medium or in the cell extract of *Streptococcus*. Furthermore, the effect of cardiolipin on enzymatic activity is distinct between mammalian HAS and streptococcal HAS (29). Although the mechanism of action of MU is complex, our results suggest that glucuronidation of MU partially accounts for the inhibition of HA synthesis in mammalian cells.

Specific inhibitors targeting HA biosynthesis may serve as useful drugs to prevent the malignant alteration of cancer or the fibrosis of organs. Clinical application of MU, based on the inhibition of HA synthesis, is feasible because this compound has been used safely for many years as a cholagogue in human medicine (27). Nevertheless, it is important to avoid the use of a very high dose of MU thereby reducing the possibility of cytotoxicity. The information presented in this report will be useful in the development of new drugs with improved efficacy. In particular, other acceptors for UGTs should be potent inhibitors of HAS activity. Further investigation will be undertaken in this regard.

Acknowledgments—We thank Drs. Andrew P. Spicer (Texas A and M University) and John A. McDonald (University of Utah) for providing mouse HAS2 cDNA. We also thank Dr. Minoru Okayama (Kyoto Sangyo University, Kyoto, Japan) for helpful comments.

REFERENCES

1. Laurent, T. C., and Fraser, J. R. E. (1992) *FASEB J.* **6,** 2397–2404
2. Knudson, C. B., and Knudson, W. (1993) *FASEB J.* **7,** 1233–1241
3. Knudson, W., Biswas, C., Li, X. Q., Nemec, R. E., and Toole, B. P. (1989) *CIBA Found. Symp.* **143,** 150–159
4. Toole, B. P., Wight, T. N., and Tammi, M. I. (2002) *J. Biol. Chem.* **277,** 4593–4596
5. Laurent, T. C., Laurent, U. B., and Fraser, J. R. (1996) *Ann. Med.* **28,** 241–253
6. Levesque, H., Girard, N., Maingonnat, C., Delpech, A., Chauzy, C., Tayot, J., Courtois, H., and Delpech, B. (1994) *Atherosclerosis* **105,** 51–62
7. Satoh, T., Ichida, T., Matsuda, Y., Sugiyama, M., Yonekura, K., Ishikawa, T., and Asakura, H. (2000) *J. Gastroenterol. Hepatol.* **15,** 402–411
8. Plebani, M., and Burlina, A. (1991) *Clin. Biochem.* **24,** 219–239
9. El Maradny, E., Kanayama, N., Kobayashi, H., Hossain, B., Khatun, S., Liping, S., Kobayashi, T., and Terao, T. (1997) *Hum. Reprod.* **12,** 1080–1088
10. Kosaki, R., Watanabe, K., and Yamaguchi, Y. (1999) *Cancer Res.* **59,** 1141–1145
11. Itano, N., Sawai, T., Miyaishi, O., and Kimata, K. (1999) *Cancer Res.* **59,** 2499–2504
12. Liu, N., Gao, F., Han, Z., Xu, X., Underhill, C. B., and Zhang, L. (2001) *Cancer Res.* **61,** 5207–5214
13. Simpson, M. A., Wilson, C. M., Furcht, L. T., Spicer, A. P., Oegema, T. R., Jr., and McCarthy, J. B. (2002) *J. Biol. Chem.* **277,** 10050–10057
14. Jacobson, A., Rahmanian, M., Rubin, K., and Heldin, P. (2002) *Int. J. Cancer* **102,** 212–219
15. Weissman, B., and Meyer, K. (1954) *J. Am. Chem. Soc.* **76,** 1753–1757
16. Tammi, M. I., Day, A. J., and Turley, E. A. (2002) *J. Biol. Chem.* **277,** 4581–4584
17. Weigel, P. H., Hascall, V. C., and Tammi, M. (1997) *J. Biol. Chem.* **272,** 13997–14000
18. Goldberg, R. L., and Toole, B. P. (1983) *J. Biol. Chem.* **258,** 7041–7046
19. Smith, T. J. (1990) *J. Clin. Endocrinol. Metab.* **70,** 655–660
20. Zaharevitz, D. W., Chisena, C. A., Duncan, K. L., August, E. M., and Cysyk, R. L. (1993) *Biochem. Mol. Biol. Int.* **31,** 627–633
21. August, E. M., Duncan, K. L., Malinowski, N. M., and Cysyk, R. L. (1993) *Oncol. Res.* **5,** 415–422
22. Ueki, N., Taguchi, T., Takahashi, M., Adachi, M., Ohkawa, T., Amuro, Y., Hada, T., and Higashino, K. (2000) *Biochim. Biophys. Acta* **1495,** 160–167
23. Nakamura, T., Takagaki, K., Shibata, S., Tanaka, K., Higuchi, T., and Endo, M. (1995) *Biochem. Biophys. Res. Commun.* **208,** 470–475
24. Nakamura, T., Funahashi, M., Takagaki, K., Munakata, H., Tanaka, K., Saito, Y., and Endo, M. (1997) *Biochem. Mol. Biol. Int.* **43,** 263–268
25. Endo, Y., Takagaki, K., Takahashi, G., Kakizaki, I., Funahashi, M., Yokoyama, M., and Endo, M. (2000) in *Progress in Transplantation* (Munakata, A., ed) pp. 1–7, Elsevier Science Publishers B. V., Amsterdam
26. Sohara, Y., Ishiguro, N., Machida, K., Kurata, H., Thant, A. A., Senga, T., Matsuda, S., Kimata, K., Iwata, H., and Hamaguchi, M. (2001) *Mol. Biol. Cell* **12,** 1859–1868
27. Takeda, S., and Aburada, M. (1981) *J. Pharmacobio-Dyn.* **4,** 724–734
28. Kakizaki, I., Takagaki, K., Endo, Y., Kudo, D., Ikeya, H., Miyoshi, T., Baggenstoss, B. A., Tlapak-Simmons V. L., Kumari, K., Nakane, A., Weigel, P. H., and Endo, M. (2002) *Eur. J. Biochem.* **269,** 5066–5075
29. Yoshida, M., Itano, N., Yamada, Y., and Kimata, K. (2000) *J. Biol. Chem.* **275,** 497–506
30. Chichibu, K., Matsuura, T., Shichijo, S., and Yokoyama, M. M. (1989) *Clin. Chim. Acta* **181,** 317–323
31. Ito, M., Yamamoto, K., Maruo, Y., Sato, H., Fujiyama, Y., and Bamba, T. (2002) *Eur. J. Clin. Pharmacol.* **58,** 11–14
32. Itano, N., Sawai, T., Yoshida, M., Lenas, P., Yamada, Y., Imagawa, M., Shinomura, T., Hamaguchi, M., Yoshida, Y., Ohnuki, Y., Miyauchi, S., Spicer, A. P., McDonald, J. A., and Kimata, K. (1999) *J. Biol. Chem.* **274,** 25085–25092
33. Knudson, W., and Knudson, C. B. (1991) *J. Cell Sci.* **99,** 227–235
34. Zimmerman, C. L., Ratna, S., Leboeuf, E., and Pang, K. S. (1991) *J. Chromatogr.* **563,** 83–94
35. Kamst, E., Bakkers, J., Quaedvlieg, N. E., Pilling, J., Kijne, J. W., Lugtenberg, B. J., and Spaink, H. P. (1999) *Biochemistry* **38,** 4045–4052
36. Kanou, M., Saeki, K., Kato, T., Takahashi, K., Mizutani, T. (2002) *Fundam. Clin. Pharmacol.* **16,** 513–517
37. Takagaki, K., Kojima, K., Majima, M., Nakamura, T., Kato, I., and Endo, M. (1992) *Glycoconj. J.* **9,** 174–179
38. Hanioka, N., Jinno, H., Tanaka-Kagawa, T., Nishimura, T., and Ando, M. (2001)) *J. Pharm. Biomed. Anal.* **25,** 65–75
39. Ciotti, M., Marrone, A., Potter, C., and Owens, I. S. (1997) *Pharmacogenetics* **7,** 485–495
40. Bock-Hennig, B. S., Kohle, C., Nill, K., and Bock, K. W. (2002) *Biochem. Pharmacol.* **63,** 123–128
41. Sobue, M., Habuchi, H., Ito, K., Yonekura, H., Oguri, K., Sakurai, K., Kamohara, S., Ueno, Y., Noyori, R., and Suzuki, S. (1987) *Biochem. J.* **241,** 591–601
42. Takagaki, K., Nakamura, T., Kon, A., Tamura, S., and Endo, M. (1991) *J. Biochem. (Tokyo)* **109,** 514–519
43. Matuoka, K., Mitsui, Y., and Murota, S. (1985) *Cell Biol. Int. Rep.* **9,** 577–586
44. Itano, N., Sawai, T., Atsumi, F., Miyaishi, O., Taniguchi, S., Kannagi, R., Hamaguchi, M., and Kimata, K. (2004) *J. Biol. Chem.* **279,** 18679–18687
45. Peng, L., Kawagoe, Y., Hogan, P., and Delmer, D. (2002) *Science* **295,** 147–150
46. Gressner, A. M. (1991) *Exp. Mol. Pathol.* **55,** 143–169
47. Gressner, A. M. (1991) *Biochem. Pharmacol.* **42,** 1987–1995
48. McCormick, C., Leduc, Y., Martindale, D., Mattison, K., Esford, L. E., Dyer, A. P., and Tufaro, F. (1998) *Nat. Genet.* **19,** 158–161
49. Lind, T., Tufaro, F., McCormick, C., Lindahl, U., and Lidholt, K. (1998) *J. Biol. Chem.* **273,** 26265–26268
50. Kitagawa, H., Uyama, T., and Sugahara, K. (2001) *J. Biol. Chem.* **276,** 38721–38726
51. Yada, T., Gotoh, M., Sato, T., Shionyu, M., Go, M., Kaseyama, H., Iwasaki, H., Kikuchi, N., Kwon, Y. D., Togayachi, A., Kudo, T., Watanabe, H., Narimatsu, H., and Kimata, K. (2003) *J. Biol. Chem.* **278,** 30235–30247
52. Yada, T., Sato, T., Kaseyama, H., Gotoh, M., Iwasaki, H., Kikuchi, N., Kwon, Y. D., Togayachi, A., Kudo, T., Watanabe, H., Narimatsu, H., and Kimata, K. (2003) *J. Biol. Chem.* **278,** 39711–39725
53. Radominska-Pandya, A., Pokrovskaya, I. D., Xu, J., Little, J. M., Jude, A. R., Kurten, R. C., and Czernik, P. J. (2002) *Arch. Biochem. Biophys.* **399,** 37–48
54. Ouzzine, M., Antonio, L., Burchell, B., Netter, P., Fournel-Gigleux, S., and Magdalou, J. (2000) *Mol. Pharmacol.* **58,** 1609–1615

THE JOURNAL OF BIOLOGICAL CHEMISTRY
© 2004 by The American Society for Biochemistry and Molecular Biology, Inc.

Vol. 279, No. 18, Issue of April 30, pp. 18920–18925, 2004
Printed in U.S.A.

In Vivo Hyaluronan Synthesis upon Expression of the Mammalian Hyaluronan Synthase Gene in *Drosophila**

Received for publication, December 30, 2003, and in revised form, February 9, 2004
Published, JBC Papers in Press, February 13, 2004, DOI 10.1074/jbc.M314293200

Satomi Takeo‡, Momoko Fujise§, Takuya Akiyama¶, Hiroko Habuchi§, Naoki Itano§, Takashi Matsuo‡, Toshiro Aigaki‡, Koji Kimata§, and Hiroshi Nakato¶‖

From the ‡Department of Biological Sciences, Tokyo Metropolitan University, Hachioji-shi, Tokyo 192-0397, Japan, the §Institute for Molecular Science of Medicine, Aichi Medical University, Nagakute, Aichi 480-1195, Japan, and the ¶Department of Genetics, Cell Biology, and Development, University of Minnesota, Minneapolis, Minnesota 55455

Hyaluronan (HA) is a large linear polymer of repeating disaccharides of glucuronic acid and GlcNAc. Although HA is widely distributed in vertebrate animals, it has not been found in invertebrates, including insect species. Insects utilize chitin, a repeating β-1,4-linked homopolymer of GlcNAc, as a major component of their exoskeleton. Recent studies illustrate the similarities in the biosynthetic mechanisms of HA and chitin and suggest that HA synthase (HAS) and chitin synthase have evolved from a common ancestral molecule. Although the biochemical properties and *in vivo* functions of HAS proteins have been extensively studied, the molecular basis for HA biosynthesis is not completely understood. For example, it is currently not clear if proper chain elongation and secretion of HA require other components in addition to HAS. Here, we demonstrate that a non-HA-synthesizing animal, the fruit fly *Drosophila melanogaster*, can produce HA *in vivo* when a single HAS protein is introduced. Expression of the mouse *HAS2* gene in *Drosophila* tissues by the Gal4/UAS (upstream activating sequence) system resulted in massive HA accumulation in the extracellular space and caused various morphological defects. These morphological abnormalities were ascribed to disordered cell-cell communications due to accumulation of HA rather than disruption of heparan sulfate synthesis. We also show that adult wings with HA can hold a high level of water. These findings demonstrate that organisms synthesizing chitin (but not HA) are capable of producing HA that is structurally and functionally relevant to that in mammals. The ability of insect cells to produce HA supports the idea that *in vivo* HA biosynthesis does not require molecules other than the HAS protein. An alternative model is that *Drosophila* cells use endogenous components of the chitin biosynthetic machinery to produce and secrete HA.

Polysaccharides are used as major structural components of animal and plant bodies. In higher vertebrates, hyaluronan (HA),[1] a high molecular mass glycosaminoglycan composed of repeating β-1,4-linked disaccharides of glucuronic acid (GlcUA) and β-1,3-linked GlcNAc, is found in the extracellular matrix in many tissues, including cartilage, synovial joint, and the vitreous of the eye (1). Despite wide distribution of HA in vertebrate animals, HA has not been found in invertebrates such as arthropod species. Instead of HA, crustaceans and arthropods produce chitin, a repeating β-1,4-linked homopolymer of GlcNAc, and deposit it in their exoskeleton. In addition, the plant cell wall is composed mainly of cellulose, β-1,4-glucan. These distinct types of polysaccharides share common important functions to determine and maintain the basic architecture of organisms, suggesting an evolutionarily conserved role of the polysaccharides as major structural constituents of multicellular organisms. Consistent with this idea, the biosynthetic mechanisms of these molecules show some intriguing similarities. All enzymes that synthesize HA, chitin, and cellulose are integral plasma membrane proteins and have the invariant amino acid residues QXXRW in their catalytic domains (2). Interestingly, one of the HA synthases (HASs), mouse HAS1, is indeed capable of synthesizing chito-oligosaccharides *in vitro* when only UDP-GlcNAc is supplied as substrate in the system (2). Based on these similarities, it has been proposed that three classes of glycosyltransferases (HASs, chitin synthases, and cellulose synthases) diverged from a common ancestral molecule.

HA is a multifunctional player in the vertebrate extracellular matrix. One of the important features of the HA network is its ability to hold a large amount of water, exhibiting viscoelastic properties. HA also directly affects cell behavior through its cell-surface receptors: CD44 (for review, see Ref. 3), RHAMM (receptor for HA-mediated motility) (4, 5), and Layilin (6). Recent studies on HASs, including molecular cloning of HAS cDNAs (7–13) and genes (14, 15) and functional analyses of each HAS gene (2, 16–20), illustrate the biological importance of HA. However, little is known about the mechanism of HA synthesis. Membrane extracts prepared from yeast cells expressing the *Xenopus HAS* (*DG42*) gene showed HA synthesizing activity *in vitro* solely in the presence of exogenously supplied substrates and magnesium ions (21). Furthermore, a purified single HAS1 protein or a *HAS1* gene product of an *in vitro* transcription/translation system has been shown to have HAS activity (2). These results indicate that the HAS protein alone can synthesize HA *in vitro* without any other protein factors. However, it is not clear whether other components are required for *in vivo* HA biosynthesis for proper chain elongation, termination, and secretion.

In this study, we demonstrate that a single mammalian HAS

* This work was supported in part by National Institutes of Health Grant HD042769 and Human Frontier Science Program Grant RGP0009/2003. The costs of publication of this article were defrayed in part by the payment of page charges. This article must therefore be hereby marked "*advertisement*" in accordance with 18 U.S.C. Section 1734 solely to indicate this fact.

‖ To whom correspondence should be addressed: Dept. of Genetics, Cell Biology, and Development, University of Minnesota, 6-160 Jackson Hall, 321 Church St. SE., Minneapolis, MN 55455. Tel.: 612-625-1727; Fax: 612-626-5652; E-mail: nakat003@umn.edu.

[1] The abbreviations used are: HA, hyaluronan; GlcUA, glucuronic acid; HAS, hyaluronan synthase; UAS, upstream activating sequence; b-HABP, biotinylated HA-binding protein.

protein (HAS2) can efficiently synthesize and secrete HA in *Drosophila*, which is a chitin-synthesizing organism and which does not naturally produce HA. This implies that conversion of the biosynthetic machinery of chitin to that of HA can happen by a single molecule exchange: substitution of chitin synthase with HAS. *HAS2* expression caused various morphological defects due to disruption of cell-cell communication. HA synthesized in fly tissues was able to retain a high level of water, which is the characteristic biophysical feature of this macromolecule. The ability of *Drosophila* cells to produce functional HA supports the idea that HAS is the only critical factor required for normal HA biosynthesis. Another interesting possibility is that HA is produced by HAS together with endogenous components involved in chitin biosynthesis.

EXPERIMENTAL PROCEDURES

Upstream Activating Sequence (UAS) Constructs and Ectopic Expression—The *UAS-HAS2* transgene was constructed by cloning the full-length mouse *HAS2* cDNA into the pUAST vector. Transgenic flies were obtained by P-element-mediated germ line transformation (22). In this study, we used two independent *HAS2* transgenic strains (*UAS-HAS2-1* and *UAS-HAS2-2*) that bear transgenic insertions at different chromosomal locations. The *HAS2* gene was misexpressed in the Gal4/UAS system (23) using the following Gal4 drivers. *29BD-GAL4* is an enhancer trap line of P{GawB} and ubiquitously expresses a high level of Gal4 protein (24). *engrailed-GAL4* and *apterous-GAL4* were used to express *HAS2* in the posterior and dorsal compartments of the wing disc, respectively. *GMR-GAL4* and *A9-GAL4* drive target gene expression in developing eyes and wings, respectively. To overexpress *sugarless* (*sgl*), we used the transgenic strain bearing the *sgl* gene under the control of the ubiquitin promoter (*ubi-sgl*) (25).

Preparation and Quantification of Glycosaminoglycans—To quantify HA and chondroitin sulfate, crude glycosaminoglycans from 25 mg of lyophilized *Drosophila* third instar larvae were prepared as described previously (26) and dissolved in 100 μl of H_2O. A 20-μl portion of the crude glycosaminoglycans was digested with 2 turbidity reducing unit of *Streptomyces* hyaluronidase in 100 μl of 50 mM acetate buffer (pH 6.0) at 60 °C for 1 h. The resulting hyaluronic acid tera- and hexasaccharides were then filtered with Ultrafree-MC (5000 nominal molecular weight limit). HA contained in the filtrates and the recovered glycosaminoglycans retained on the filter were digested separately with chondroitinases ABC and ACII and 5 μg of bovine serum albumin in 50 μl of 50 mM Tris-HCl (pH 8) at 37 °C for 2 h. The digests were filtered with Ultrafree-MC (5000 nominal molecular weight limit), and unsaturated disaccharides contained in the filtrates were determined by reversed-phase ion pair chromatography using a Senshu-Pak Docosil column equipped with a post-column fluorescence detector according to the method of Toyoda *et al.* (26) except for a slight modification of the elution conditions.

For preparation and quantification of heparan sulfate, a 10-μl portion of the crude glycosaminoglycans was digested with a mixture of 10 milliunits of heparitinase I, 5 milliunits of heparitinase II, and 10 milliunits of heparitinase III in 50 μl of 50 mM Tris-HCl (pH 7.2), 1 mM $CaCl_2$, and 4 μg of bovine serum albumin at 37 °C for 16 h. The digests were analyzed as described above.

Preparation and Quantification of Chitin—For the quantitative measurement of chitin, the amount of GlcNAc released by chitinase was measured by a colorimetric method. Lyophilized *Drosophila* larvae (25 mg, dry weight) were homogenized with 1.0 ml of acetone. The homogenate was washed with acetone and dried. The pellet was suspended in 1.0 ml of 0.1 N NaOH for 16 h at room temperature. After alkali treatment, 25 μl of 4 N acetic acid were added; actinase E was then added and incubated at 37 °C for 2 h. Insoluble material was isolated by centrifugation, washed twice with water, and resuspended in 400 μl of 200 mM acetate buffer (pH 5.0). Chitinase (2.0 mg) from *Bacillus* sp. dissolved in the same buffer (200 mM) was added, and the mixed solution was incubated at 37 °C for 90 min. After centrifugation, an 80-μl aliquot of each sample was assayed for GlcNAc by measuring the absorbance at 585 nm (27).

Agarose Gel Electrophoresis of HA—A 20-μl portion of the crude glycosaminoglycans prepared as described above was fractionated by 0.5% agarose gel electrophoresis (28). After electrophoresis, HA was blotted onto nylon membrane and detected by the ECL detection system with biotinylated HA-binding protein (b-HABP) (Seikagaku Co.) as a probe as described previously (17). HA with average masses of 21.3, 14.1, 9.9, 6.4, 4.6, and 1.0×10^6 Da was used as a standard.

To test the sensitivity of detected bands to chitinase and hyaluronidase, the crude glycosaminoglycan fractions were treated with these enzymes before gel electrophoresis. The samples were incubated with 0.5 mg of chitinase from *Bacillus* sp. at 37 °C for 90 min (29). After inactivation of chitinase by heating at 95 °C for 5 min, glycosaminoglycans were recovered by ethanol precipitation. Subsequently, the samples were incubated with or without 0.1 turbidity reducing unit of *Streptomyces* hyaluronidase at 55 °C for 1 h.

Histochemical Staining—To detect HA *in situ* in *Drosophila* tissues, histochemical staining was performed using b-HABP as a probe (17). Wing imaginal discs were dissected from third instar larvae and fixed with 4% formaldehyde in phosphate-buffered saline for 50 min. Endogenous peroxidase activity was quenched with 0.3% H_2O_2 in methanol. After washing with 0.3% Triton X-100 in phosphate-buffered saline, nonspecific binding was blocked with 10% goat serum in 0.3% Triton X-100 in phosphate-buffered saline. The discs were incubated with 2.5 μg/ml b-HABP in 10% goat serum overnight at 4 °C. After unbound probe was washed off, the discs were incubated with Avidin-Biotin Complex regent (Vector Labs, Inc.) for 1 h, and b-HABP was detected by staining with 0.5 mg/ml 3,3′-diaminobenzidine and 0.03% H_2O_2 diluted in phosphate-buffered saline. For subcellular localization of HA, the signal was amplified and detected using a tyramide signal amplification fluorescence system (PerkinElmer Life Sciences) and imaged using an LSM410 confocal microscope (Carl Zeiss, Inc.). Cobalt sulfide staining was performed to visualize the apical surface of pupal retina as described previously (30).

Quantification of the H_2O Content of Drosophila Adult Wings—Adult wings were collected from wild-type or *29BD-GAL4/UAS-HAS2-2* males at 3–5 days after eclosion. To prevent evaporation of water from the tissue, wings were rapidly removed from the thorax at the base using forceps. Approximately 25–50 wings (0.1–0.2 mg) were used as a sample to measure the H_2O content by the coulometric Karl-Fischer method (31, 32) using an AQ-6 water content analyzer (Hiranuma Sangyo Co.). Immediately after the fresh weight of each sample was determined using an S4 Ultramicro balance (Sartorius Corp.), water was extracted from the wings and titrated with Hydranal Aqualyte RS (Riedel-deHaen Co.) as a titrant. Aqualyte CN (Kanto Kagaku Co.) was used as a solvent. Sets of four and six samples were prepared for wild-type and *29BD-GAL4/UAS-HAS2-2* wings, respectively, and measurements were performed independently.

RESULTS

HA Synthesis upon HAS2 Expression in Drosophila—A previous biochemical study on glycosaminoglycans from *Drosophila* showed that no detectable HA exists in this organism (26). We first asked whether *Drosophila* cells have the ability to synthesize HA when a HAS protein is introduced. We used the Gal4/UAS system (23) to drive expression of the mouse *HAS2* gene *in vivo*. The *HAS2* cDNA was ligated downstream of the UAS, and the resultant plasmid construct was integrated into the genomic DNA by P-element-mediated transformation. The established *Drosophila* strains bearing the *UAS-HAS2* transgene were crossed with various Gal4 strains to express HAS genes ubiquitously or in a tissue-specific manner. To determine whether HA is synthesized in the HAS gene-expressing animals, we prepared crude glycosaminoglycan fractions from third instar larvae according to the method described previously (26) and quantified HA. A large amount of HA was detected in larvae obtained from crosses between the *29BD-GAL4* driver and two independent *UAS-HAS2* transgenic strains, whereas no detectable HA was observed in the wild-type control animals (Table I).

We also examined HA synthesis *in situ* using b-HABP as a probe. *HAS2* expression was induced by *engrailed-GAL4*, which drives Gal4 expression in the posterior compartment of imaginal discs (Fig. 1*A*). Histochemical staining showed specific binding of the b-HABP probe to the posterior half of the wing (Fig. 1*B*). This result confirmed that HA is synthesized in *Drosophila* tissues and accumulates at the sites of *HAS2* expression. We also used this probe in a fluorescence detection system to determine the subcellular localization of HA. As shown in Fig. 1*C*, signals were detected mainly on the cell

TABLE I

Determination of the amounts of glycosaminoglycans and chitin from HAS2-transgenic Drosophila

Crude glycosaminoglycans were prepared from wild-type and *29BD)HAS2* third instar larvae. The amounts of HA, chondroitin sulfate (CS), and heparan sulfate (HS) were determined by fluorescence disaccharide analysis. Chitin was also quantified as described under "Experimental Procedures." Two independent transgenic strains for *UAS-HAS2* (*UAS-HAS2-1* and *UAS-HAS2-2*) were used for this analysis. ND, not detectable.

Genotype	HA	CS	HS	Chitin
	nmol/mg (dry weight)	*nmol/mg (dry weight)*	*nmol/mg (dry weight)*	*pmol/mg (dry weight)*
Wild-type	ND	0.54	0.14	5.8
29BD)HAS2-1	0.20	0.54	0.10	5.6
29BD)HAS2-2	0.04	0.56	0.14	5.4

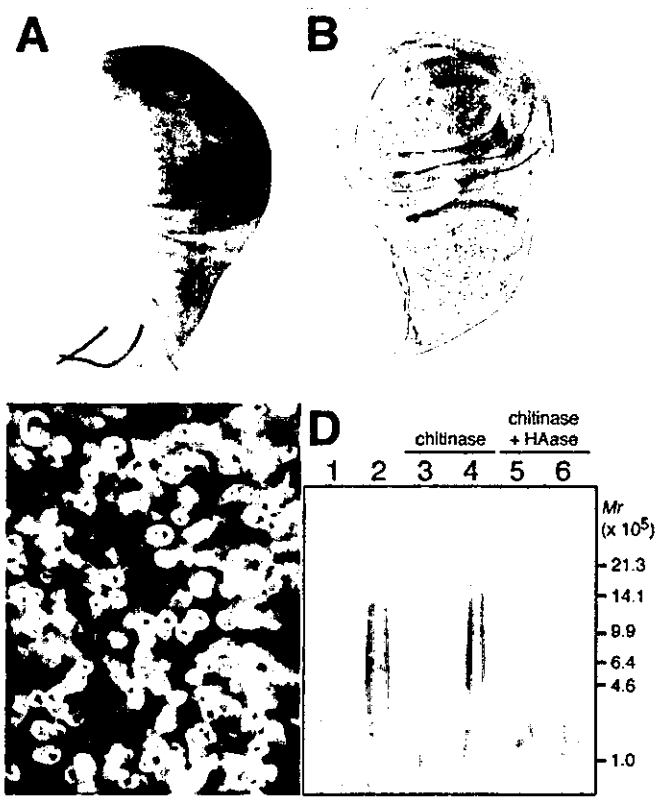

FIG. 1. **HA synthesis upon mouse *HAS2* expression in *Drosophila* wing discs.** *A*, the posterior compartment-specific pattern of *engrailed-GAL4* expression in the wing disc. The expression pattern of *lacZ* in *engrailed-GAL4/UAS-lacZ* wing discs was monitored by β-galactosidase activity staining. *B*, HA localization in the *engrailed-GAL4/UAS-HAS2-2* wing disc determined by staining using b-HABP as a probe. HA was specifically detected in the posterior region where *HAS2* was overexpressed by *engrailed-GAL4*. *C*, subcellular localization of HA in the *HAS2*-expressing disc. The fluorescent signal of HA was detected on the cell surface and/or in the extracellular space. *D*, agarose gel electrophoresis of HA synthesized in *Drosophila*. Crude glycosaminoglycan fractions were prepared from wild-type (*lanes 1*, *3*, and *5*) and *29BD-GAL4/UAS-HAS2-2* (*lanes 2*, *4*, and *6*) animals as described under "Experimental Procedures" and separated by agarose gel electrophoresis. Samples loaded in *lanes 3* and *4* were treated with chitinase (from *Bacillus* sp.) before gel electrophoresis; those loaded in *lanes 5* and *6* were digested with both chitinase and *Streptomyces* hyaluronidase (HAase). HA was blotted onto nylon membrane and detected using the ECL detection system with b-HABP as a probe. HA with average masses of 21.3, 14.1, 9.9, 6.4, 4.6, and 1.0 × 10^5 Da was used as a standard.

surface, suggesting that synthesized HA is secreted and deposited on the cell surface or in the extracellular matrix.

We next analyzed the size distribution of HA synthesized in the *HAS2* transgenic animals. Crude glycosaminoglycan fractions prepared from wild-type and *29BD-GAL4/UAS-HAS2* larvae were separated by agarose gel electrophoresis. HA was blotted onto nylon membrane and detected using b-HABP as a probe. In the crude glycosaminoglycan preparation from *HAS2*-expressing animals, we detected HA, which migrated as broad peaks with large molecular masses ranging from 1 × 10^5 to 2 × 10^6 Da (Fig. 1*D*, *lane 2*). The size distribution of HA prepared from *29BD-GAL4/UAS-HAS2* animals was smaller than that synthesized by the same enzyme in rat 3Y1 fibroblasts (molecular masses of >2 × 10^6 Da), but was comparable with that produced *in vitro* by membrane preparation of HAS2 transfectant (molecular masses of 2 × 10^5 to 2 × 10^6 Da) (17). On the other hand, a weak background signal was observed at a low molecular mass range in the wild-type control lane (Fig. 1*D*, *lane 1*). To determine whether this low molecular mass smear band reflects the existence of HA or other related molecules in the wild-type fraction, we tested its sensitivity to chitinase (*Bacillus*) and hyaluronidase (*Streptomyces*). As shown in *lanes 3* and *5*, the low molecular mass signals were not eliminated by incubation with chitinase or hyaluronidase, indicating that these signals do not represent either HA or chitin. In contrast, HA produced in *HAS2*-expressing animals was not affected by chitinase treatment (*lane 4*), but was completely degraded by adding hyaluronidase (*lane 6*). Although the nature of the low molecular mass band is unknown, it seems to be a background signal detectable only in blotting experiments because the b-HABP probe specifically recognized regions of the wing discs where *HAS2* was expressed *in situ* (Fig. 1*B*) and did not stain wild-type discs (data not shown).

HAS2 Gene Expression Disrupts Morphogenesis in Drosophila Tissues—Overexpression of *HAS2* using several different Gal4 drivers caused lethality and a variety of morphological defects in adult tissues (Fig. 2). Eye-specific expression of the *HAS2* gene by *GMR-GAL4* induced a so-called "rough eye" phenotype, characterized by reduced numbers of ommatidia and disordered ommatidial arrays of the compound eye (Fig. 2*B*). To further analyze this eye defect, we observed pupal retina stained with cobalt sulfide (Fig. 2, *C* and *D*). In contrast to wild-type retina, which showed precise and ordered patterns of differentiation of ommatidial components, *HAS2*-expressing eyes exhibited several distinct defects. These abnormalities included decreased numbers of cone cells, abnormal sizes and shapes of primary pigment cells, and ectopic interommatidial bristles. Overexpression of *HAS2* in the developing wing using *A9-GAL4* led to thickened and disarranged wing veins (Fig. 2, *E* and *F*). When *HAS2* expression was induced in the dorsal part of wing imaginal discs by *apterous-GAL4*, the wings failed to extend. In addition, the patterns and formation of notal bristles were disrupted; most large mechanosensory bristles (macrochaetae) were lost or shortened with abruptly ended tips (Fig. 2, *G* and *H*). In this study, we used two independent *HAS2* transgenic strains, *UAS-HAS2-1* and *UAS-HAS2-2*. The phenotypes associated with *HAS2* expression by these two transgenes were fundamentally similar, but different in severity (Table II). Expression of *UAS-HAS2-1*, which produces higher levels of HA, resulted in more severe expressivity and higher penetrance compared with that of *UAS-HAS2-2*.

All these abnormalities are known to be caused by defective intercellular signaling. For example, during eye development, differentiation of cone and pigment cells requires activation of the *Drosophila* epidermal growth factor receptor (DER), and

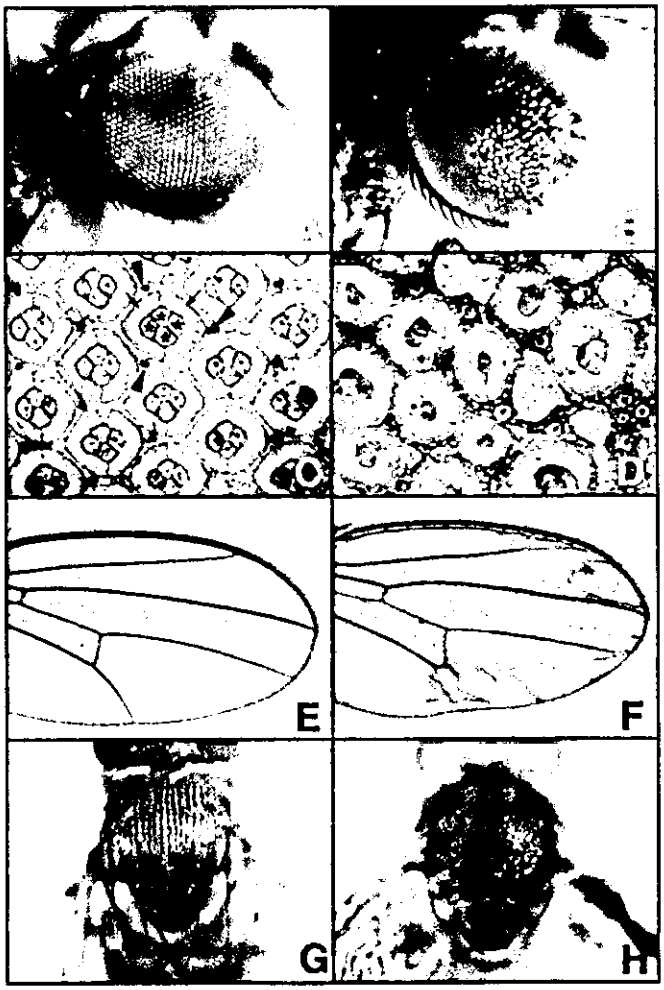

FIG. 2. **Expression of the *HAS2* gene disrupts normal morphogenesis in *Drosophila* tissues.** *A–D*, effect of *HAS2* expression on eye morphogenesis. Adult eyes (*A* and *B*) and pupal eyes stained with cobalt sulfide (*C* and *D*) are shown for wild-type animals (*A* and *C*) and animals with *HAS2*-expression by *GMR-GAL4* (*B* and *D*). Cone cells (*asterisks*), pigment cells (*arrows*), and bristles (*arrowheads*) are shown. *E* and *F*, wild-type and *A9-GAL4/UAS-HAS2-1* wings, respectively. *G* and *H*, effect of *HAS2* overexpression in the dorsal compartment of the wing disc. Wild-type and *UAS-HAS2-1/+;apterous-GAL4/+* dorsal thoraxes are shown, respectively.

compromising DER signaling leads to reduced numbers of cone cells and pigment cells (33). On the other hand, an enlarged wing vein is a common phenotype observed upon reduction of Notch signaling (34, 35). In addition, the bristle phenotypes of *UAS-HAS2/+;apterous-GAL4/+* flies resemble those of *warthog* (*wrt*) mutants (36). The *wrt* gene encodes a *Drosophila* homolog of Rab6, which regulates trafficking from the Golgi to the *trans*-Golgi network, and is required for proper secretion and cell-surface presentation of extracellular or transmembrane proteins. One of the signaling cascades affected by *wrt* mutations is the Notch pathway (37). It is therefore possible that some of *HAS2* overexpression phenotypes are a result of altered DER and/or Notch pathways. This observation suggests that *HAS2* expression interferes with cell-cell communications required for normal cell growth and differentiation during *Drosophila* tissue assembly.

HAS2 Expression Does Not Affect the Levels of Other Glycosaminoglycans and Chitin—Are the morphological defects of the *HAS2*-expressing animals caused by HA deposition? Alternatively, does *HAS2* expression affect the levels of other polysaccharides and therefore indirectly produce the phenotypes? In particular, because the biosynthesis of HA and heparan sulfate, a different class of glycosaminoglycans, requires the common substrates UDP-GlcUA and UDP-GlcNAc, a possible explanation for these phenotypes could be interference with heparan sulfate synthesis; high levels of HAS protein may compete for the substrates with the endogenous heparan sulfate biosynthetic machinery. Indeed, a number of studies have demonstrated that heparan sulfate plays a critical role in *Drosophila* morphogenesis (for reviews, see Refs. 38–41). Similarly, synthesis of chondroitin sulfate and chitin, which need UDP-GlcUA and UDP-GlcNAc, respectively, may also be affected. To determine the effects of *HAS2* expression on the biosynthesis of chondroitin sulfate, heparan sulfate, and chitin, we measured the levels of these polysaccharides in the *HAS2*-expressing animals. As shown in Table I, we did not detect a significant change in the levels of these molecules upon expression of *HAS2*, although *UAS-HAS2-1/+;29BD-GAL4/+* showed a moderately reduced level of heparan sulfate.

Overexpression of UDP-glucose Dehydrogenase Enhances the Phenotype of HAS2-expressing Animals—Several lines of information suggest that the moderate reduction of heparan sulfate in *UAS-HAS2-1/+;29BD-GAL4/+* animals is unlikely to cause the morphological defects in the *HAS2*-expressing animals. First, reduced levels of heparan sulfate cannot explain the various phenotypes of *29BD-GAL4/UAS-HAS2-2*, which showed a normal level of heparan sulfate (Table I). Second, we have several other transgenic strains that produce higher levels of HA and also show wild-type levels of heparan sulfate (data not shown); thus, HA production and heparan sulfate reduction do not seem to be directly correlated. To further examine whether the phenotypes associated with *HAS2* expression depend on the levels of HA or heparan sulfate, we performed a sensitive genetic assay in which the cellular levels of UDP-GlcUA were manipulated. If the *HAS2* overexpression phenotypes are caused by HA accumulation on the cell surface, these phenotypes should be enhanced by increasing the UDP-GlcUA level and should be suppressed by its reduction. The reverse will happen if these defects are consequences of loss of substrates and defective heparan sulfate-dependent signaling. Based on these criteria, we genetically manipulated the dosage of *sgl*, which encodes a UDP-glucose dehydrogenase, an essential enzyme for UDP-GlcUA biosynthesis (25, 42–45), and examined its effect on the rough eye phenotype of *GMR-GAL4/+; UAS-HAS2/+* animals. As depicted in Fig. 3*B*, we did not detect a significant change in the phenotype by deleting one copy of *sgl*. On the other hand, overexpression of *sgl* by the transgene under the control of the ubiquitin promoter (*ubi-sgl*) (25) dramatically enhanced the eye defects, resulting in gross defects in eye formation with necrosis (Fig. 3*D*). This observation indicates that HA accumulation (but not disrupted heparan sulfate synthesis) is responsible for the morphological abnormalities in the *HAS2*-expressing animals.

HA-synthesizing Wings Accumulate High Levels of Water—The ability of HA to hold a large amount of water is an important biophysical property as a structural constituent of the extracellular matrix. We noticed that *HAS2* overexpression by the *UAS-HAS2-2* transgene under the control of *29BD-GAL4* at 20 °C induced the characteristic wing phenotypes (Fig. 4, *B* and *B'*). These wings were thick and partly wrinkled, and the dorsal and ventral epithelial sheets were detached from each other. In addition, they were opaque compared with wild-type wings, which were transparent. Overall, the wings appeared to be swollen with fluid in their interior. Wings from *engrailed-GAL4/+;UAS-HAS2-2/+* adults also exhibited a similar phenotype only in the posterior compartment (data not shown), confirming that this phenotype is associated with HA accumulation. To determine whether these wings show in-

TABLE II

Phenotypes produced by expression of the HAS2 gene in Drosophila

The phenotypes induced by *HAS2* expression by two independent transgenic strains (*UAS-HAS2-1* and *UAS-HAS2-2*) with each GAL4 driver are shown. Expression of *UAS-HAS2-1*, which produces higher levels of HA, resulted in much more severe phenotypes compared with that of *UAS-HAS2-2*. Corresponding figures are shown in parentheses.

GAL4 lines	Expression	*UAS-HAS2-1*	*UAS-HAS2-2*
Actin 5C	Ubiquitous	Lethality (first instar larval stage)	Lethality (pupal stage)
29BD	Ubiquitous	Lethality (pupal stage)	Disordered wing veins, wet wing, eclosion defect (Fig. 4)
GMR	Eye disc	Severe rough eye	Mild rough eye (Fig. 3*A*)
A9	Wing and halter discs	Thickened and ectopic veins, extra notal bristles (Fig. 2*F*)	Disordered veins
apterous	Dorsal compartment of wing disc	Semilethality, eclosion defect, folded wing, abnormal shape and patterns of notal bristles (Fig. 2*H*)	Disordered veins
engrailed	Posterior compartment	Eclosion defect, folded wing	Disordered veins, wet wing

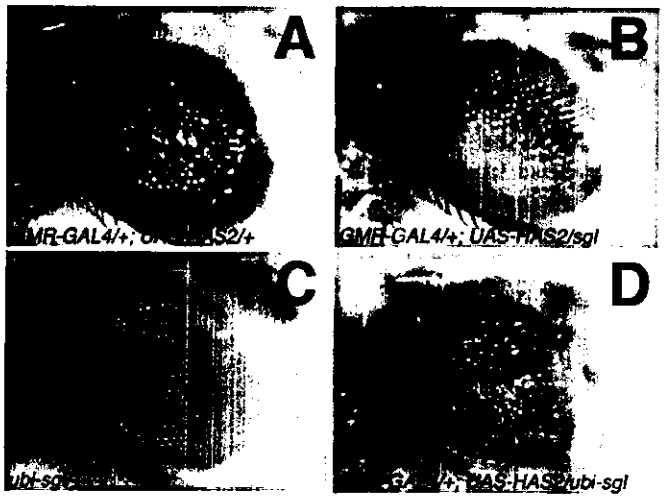

FIG. 3. **Overexpression of *sgl* enhances the eye phenotype of *HAS2*-expressing animals.** Adult eyes are shown for *GMR-GAL4/+; UAS-HAS2-2/+* (*A*), *GMR-GAL4/+;UAS-HAS2-2/sgl* (*B*), *ubi-sgl/+* (*C*), and *GMR-GAL4/+;UAS-HAS2-2/ubi-sgl* (*D*). Deleting one copy of the *sgl* gene did not affect the eye phenotype of *HAS2*-expressing animals. On the other hand, this phenotype was drastically enhanced by ubiquitous overexpression of *sgl*.

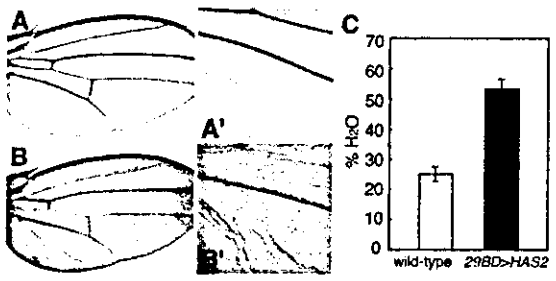

FIG. 4. ***Drosophila* wings synthesizing HA show high water content.** Wings are shown for wild-type (*A* and *A'*) and *29BD-GAL4/UAS-HAS2-2* (*B* and *B'*) animals. *A'* and *B'* are high magnification views of *A* and *B*, respectively. In *C*, the water content of adult wings was determined by the coulometric Karl-Fischer method (31, 32). Each *error bar* represents the S.E. of four and six measurements of wild-type and *29BD-GAL4/UAS-HAS2-2* wings, respectively. The difference among them is significant at the 1% level as determined by Mann-Whitney's *U* test ($p = 0.0089$).

creased water content, we collected wild-type and *29BD-GAL4/UAS-HAS2-2* wings and measured H_2O in these tissues by the Karl-Fischer titration, a well established method for determining water (31, 32). Indeed, the water content of wings that produced HA was considerably high, reaching twice as much as that of the wild-type wings (Fig. 4*C*). We therefore call this phenotype "wet wing" in Table II. Thus, HA synthesized in *Drosophila* wing cells is capable of holding a high level of water and is likely to be functionally relevant to that synthesized in mammalian cells.

DISCUSSION

Insects produce cuticle, the chitin-based exoskeleton that prevents desiccation of body moisture. This structure enables these species to attain light body weight and to accommodate a large variety of living space. On the other hand, higher vertebrate animals employ HA, which ensures water inside the body. Thus, the life styles of animals are not unrelated to the polysaccharides they produce, and diversion of HA- and chitin-producing organisms could be one of the key steps in animal evolution. Recent studies suggest that the HAS and chitin synthase genes have evolved from a common origin. Here, we have provided evidence that HA can be produced by introducing a single HAS gene into a chitin-synthesizing multicellular organism, the *Drosophila* fruit fly, which normally does not synthesize HA. The HAS2 enzyme was active in such a heterologous system and efficiently synthesized a high level of HA without exogenously supplied substrates or primers. The observation that HA products were deposited on the cell surface implies that HAS acts in *Drosophila* cells as it functions in mammalian cells: it polymerizes HA chains at the inner face of the plasma membrane and coordinately secretes HA out of the cell. This result is significant because it is currently unclear whether proper elongation and secretion of HA require other proteinaceous and non-proteinaceous components in addition to HAS. Our finding of efficient HA production and secretion in insect cells strongly supports that such additional factors are not essential for normal HA biosynthesis. However, we cannot exclude the possibility that HAS2 accomplishes HA synthesis by utilizing the chitin biosynthetic machinery in *Drosophila* cells. Additional studies on the biosynthetic machineries of HA and chitin will clarify this point. Thus, the *Drosophila* system will provide new insights into unsolved problems regarding HA biosynthesis.

The *HAS2*-overexpressing flies showed a variety of phenotypes in many tissues. The biochemical and genetic experiments showed that these phenotypes are caused by accumulation of HA in tissues, but not by lack of chondroitin sulfate, heparan sulfate, or chitin. How did HA synthesis induce such phenotypes? In the HA network in a physiological solution, diffusion rates of macromolecules such as proteins are expected to be slow, and the concentration of these molecules will be lower in the network compared with an HA-free environment. This would explain the observed morphological defects. The abnormalities caused by *HAS2* expression are reminiscent of phenotypes caused by disruption of intercellular signaling mediated by extracellular or cell-surface signaling molecules, the movement of which will be restricted in the HA network. For

example, disruption of diffusion of Spitz, a secreted ligand of DER, may result in a similar phenotype compared with that of *HAS2* overexpression (33). Another explanation for these phenotypes is that a particular signaling pathway is ectopically activated by HA in *Drosophila* cells. Recent mounting evidence suggests that HA triggers multiple signaling pathways (for review, see Ref. 46), and counterparts of many of these signaling components exist in flies. It is therefore possible that synthesized HA abnormally activates such cascade(s) and interferes with normal morphogenesis. Finally, some of the phenotypes appear to be a direct result of the biophysical property of HA itself. Interestingly, quantification of the water content of *Drosophila* tissues with or without HA revealed that HA produced in *Drosophila* cells shows hydrodynamic properties relevant to those of mammalian HA; HA created a new extracellular matrix, which was swollen with water.

The eye phenotype of *HAS2*-overexpressing animals was strongly enhanced by coexpression of the *sgl* gene, which encodes a UDP-glucose dehydrogenase. It is worth noting that a substantial effect of increasing the level of UDP-glucose dehydrogenase on the phenotype is consistent with the prediction that substrate availability is a limiting factor in HA biosynthesis (44). Although we have not tested the effects of alterations in UDP-GlcNAc levels on HA deposition, it is possible that the cytosolic concentration of UDP-GlcNAc might be high in insect cells that synthesize chitin, a GlcNAc polymer, at the inner face of the plasma membrane and is therefore less critical than the UDP-GlcUA level.

The consequences of lack or elevation of HA synthesis have become the recent focus of intense research interest. Camenisch *et al.* (18) showed that *HAS2*-deficient mice exhibit serious cardiovascular defects. An explant system using *HAS2*$^{-/-}$ tissue was used to demonstrate that HA is essential for a cell migration event required for cardiac cushion morphogenesis. Interestingly, ectopic deposition of HA also affects cell migration and adhesion (20). Stable HAS transfectants in non-transformed rat 3Y1 cells show reduced contact inhibition of cell growth and migration. HA overproduction in these cells also alters the microfilament organization and N-cadherin distribution at the intercellular boundaries. These phenotypes are suppressed by treatment with inhibitors of phosphatidylinositol 3-kinase, suggesting that phosphatidylinositol 3-kinase signaling mediates the HA-dependent aberration of contact inhibition. This line of studies will further improve our understanding of HA functions in cell behavior and signaling. Our present study illustrates the possibility that a model system using the genetically tractable organism *Drosophila* could be a strategy to study *in vivo* roles as well as evolution of the biosynthetic machinery of polysaccharides. Furthermore, given that insect cells are cheap and easy to handle, the fact that these cells can produce HA without any exogenous supply of donor substrates will be useful information for medical and pharmaceutical applications of HA.

Acknowledgments—We thank J. A. McDonald (Mayo Clinic, Scottsdale, AZ) for the kind gift of the mouse *HAS2* cDNA. We are grateful to M. B. O'Connor and the Bloomington Stock Center for fly stocks. We also thank F. Kato, M. Suzuki, and N. Sugiura (Seikagaku Co.) for assistance in quantification of the water content of *Drosophila* adult wings by the Karl-Fischer method.

REFERENCES

1. Toole, B. P. (1990) *Curr. Opin. Cell Biol.* **2,** 839–844
2. Yoshida, M., Itano, N., Yamada, Y., and Kimata, K. (2000) *J. Biol. Chem.* **275,** 497–506
3. Isacke, C. M., and Yarwood, H. (2002) *Int. J. Biochem. Cell Biol.* **34,** 718–721
4. Turley, E. A. (1992) *Cancer Metastasis Rev.* **11,** 21–30
5. Turley, E. A., Noble, P. W., and Bourguignon, L. Y. (2002) *J. Biol. Chem.* **277,** 4589–4592
6. Bono, P., Rubin, K., Higgins, J. M., and Hynes, R. O. (2001) *Mol. Biol. Cell* **12,** 891–900
7. Itano, N., and Kimata, K. (1996) *J. Biol. Chem.* **271,** 9875–9878
8. Shyjan, A. M., Heldin, P., Butcher, E. C., Yoshino, T., and Briskin, M. J. (1996) *J. Biol. Chem.* **271,** 23395–23399
9. Itano, N., and Kimata, K. (1996) *Biochem. Biophys. Res. Commun.* **222,** 816–820
10. Spicer, A. P., Augustine, M. L., and McDonald, J. A. (1996) *J. Biol. Chem.* **271,** 23400–23406
11. Watanabe, K., and Yamaguchi, Y. (1996) *J. Biol. Chem.* **271,** 22945–22948
12. Fulop, C., Salustri, A., and Hascall, V. C. (1997) *Arch Biochem. Biophys.* **337,** 261–266
13. Spicer, A. P., Olson, J. S., and McDonald, J. A. (1997) *J. Biol. Chem.* **272,** 8957–8961
14. Spicer, A. P., Seldin, M. F., Olsen, A. S., Brown, N., Wells, D. E., Doggett, N. A., Itano, N., Kimata, K., Inazawa, J., and McDonald, J. A. (1997) *Genomics* **41,** 493–497
15. Spicer, A. P., and McDonald, J. A. (1998) *J. Biol. Chem.* **273,** 1923–1932
16. Itano, N., Sawai, T., Miyaishi, O., and Kimata, K. (1999) *Cancer Res.* **59,** 2499–2504
17. Itano, N., Sawai, T., Yoshida, M., Lenas, P., Yamada, Y., Imagawa, M., Shinomura, T., Hamaguchi, M., Yoshida, Y., Ohnuki, Y., Miyauchi, S., Spicer, A. P., McDonald, J. A., and Kimata, K. (1999) *J. Biol. Chem.* **274,** 25085–25092
18. Camenisch, T. D., Spicer, A. P., Brehm-Gibson, T., Biesterfeldt, J., Augustine, M. L., Calabro, A., Jr., Kubalak, S., Klewer, S. E., and McDonald, J. A. (2000) *J. Clin. Investig.* **106,** 349–360
19. Camenisch, T. D., Schroeder, J. A., Bradley, J., Klewer, S. E., and McDonald, J. A. (2002) *Nat. Med.* **8,** 850–855
20. Itano, N., Atsumi, F., Sawai, T., Yamada, Y., Miyaishi, O., Senga, T., Hamaguchi, M., and Kimata, K. (2002) *Proc. Natl. Acad. Sci. U. S. A.* **99,** 3609–3614
21. DeAngelis, P. L., and Achyuthan, A. M. (1996) *J. Biol. Chem.* **271,** 23657–23660
22. Rubin, G. M., and Spradling, A. C. (1982) *Science* **218,** 348–353
23. Brand, A. H., and Perrimon, N. (1993) *Development* **118,** 401–415
24. Toba, G., Ohsako, T., Miyata, N., Ohtsuka, T., Seong, K. H., and Aigaki, T. (1999) *Genetics* **151,** 725–737
25. Haerry, T. E., Heslip, T. R., Marsh, J. L., and O'Connor, M. B. (1997) *Development* **124,** 3055–3064
26. Toyoda, H., Kinoshita-Toyoda, A., and Selleck, S. B. (2000) *J. Biol. Chem.* **275,** 2269–2275
27. Reissig, J. L., Storminger, J. L., and Leloir, L. F. (1955) *J. Biol. Chem.* **217,** 959–966
28. Lee, H. G., and Cowman, M. K. (1994) *Anal. Biochem.* **219,** 278–287
29. Zhang, M., Haga, A., Sekiguchi, H., and Hirano, S. (2000) *Int. J. Biol. Macromol.* **27,** 99–105
30. Wolff, T., and Ready, D. F. (1991) *Development* **113,** 825–839
31. Fischer, K. A. (1935) *Angew. Chem. Int. Ed. Engl.* **48,** 394–396
32. Thiex, N. J., and Van Erem, T. (2002) *J. Assoc. Off. Anal. Chem. Int.* **85,** 318–327
33. Freeman, M. (1996) *Cell* **87,** 651–660
34. de Celis, J. F., Bray, S., and Garcia-Bellido, A. (1997) *Development* **124,** 1919–1928
35. Huppert, S. S., Jacobsen, T. L., and Muskavitch, M. A. (1997) *Development* **124,** 3283–3291
36. Purcell, K., and Artavanis-Tsakonas, S. (1999) *J. Cell Biol.* **146,** 731–740
37. Verheyen, E. M., Purcell, K. J., Fortini, M. E., and Artavanis-Tsakonas, S. (1996) *Genetics* **144,** 1127–1141
38. Bernfield, M., Gotte, M., Park, P. W., Reizes, O., Fitzgerald, M. L., Lincecum, J., and Zako, M. (1999) *Annu. Rev. Biochem.* **68,** 729–777
39. Lander, A. D., and Selleck, S. B. (2000) *J. Cell Biol.* **148,** 227–232
40. Selleck, S. B. (2000) *Trends Genet* **16,** 206–212
41. Perrimon, N., and Bernfield, M. (2000) *Nature* **404,** 725–728
42. Binari, R. C., Staveley, B. E., Johnson, W. A., Godavarti, R., Sasisekharan, R., and Manoukian, A. S. (1997) *Development* **124,** 2623–2632
43. Hacker, U., Lin, X., and Perrimon, N. (1997) *Development* **124,** 3565–3573
44. Spicer, A. P., Kaback, L. A., Smith, T. J., and Seldin, M. F. (1998) *J. Biol. Chem.* **273,** 25117–25124
45. Walsh, E. C., and Stainier, D. Y. (2001) *Science* **293,** 1670–1673
46. Lee, J. Y., and Spicer, A. P. (2000) *Curr. Opin. Cell Biol.* **12,** 581–586

Differential Regulation by IL-1β and EGF of Expression of Three Different Hyaluronan Synthases in Oral Mucosal Epithelial Cells and Fibroblasts and Dermal Fibroblasts: Quantitative Analysis Using Real-Time RT-PCR

Yoichi Yamada,*† Naoki Itano,† Ken-ichiro Hata,* Minoru Ueda,‡ and Koji Kimata†

*Center for Genetic and Regenerative Medicine, Nagoya University School of Medicine, Nagoya, Japan; †Institute for Molecular Science of Medicine, Aichi Medical University, Aichi, Japan; ‡Department of Oral and Maxillofacial Surgery, Nagoya University Graduate School of Medicine, Nagoya, Japan

Using "real-time RT-PCR", we assessed the expression of three different hyaluronan synthase genes, *HAS1*, *HAS2*, and *HAS3*, by measuring their mRNA amounts in cultured human oral mucosal epithelial (COME) cells, oral mucosal fibroblasts, and dermal fibroblasts, and investigated the effects of interleukin-1β (IL-1β) and epidermal growth factor (EGF). When COME cells were treated with IL-1β or EGF, early and marked increases and subsequent rapid decreases were observed for all HAS genes and, moreover, actual changes in hyaluronan synthesis subsequently occurred. The effects of IL-1β stimulation were concentration-dependent and the maximal response to the EGF stimulation was observed at a low concentration (0.1 ng per mL). When two different types of fibroblasts were treated with IL-1β or EGF, increased expression with different degrees and rates of three different HAS genes and subsequent increased synthesis of hyaluronan were also observed. In addition, HAS1 gene expression was not detectable in the mucosal fibroblasts, while weak HAS3 gene expression was detected in the dermal fibroblasts. Taken together, it is likely that the regulation of the expression of the three different HAS genes is different between oral mucosa and skin, which may be of significance for elucidating some of the differences between these tissues in wound healing.

Key words: hyaluronan/hyaluronan synthase genes/real-time RT-PCR analysis/tissue engineering
J Invest Dermatol 122:631–639, 2004

The process of wound healing depends upon a variety of interactions between cells and the extracellular matrix (Clark and Henson, 1988). It is well known that hyaluronan not only supports tissue architecture as a passive structural component of the matrix in various connective tissues but is also involved in dynamic cellular processes such as cell migration and cell–cell recognition during wound healing and inflammation (Weigel *et al*, 1997; Knudson *et al*, 1989; Turley, 1989). Three different mammalian hyaluronan synthases, HAS1, HAS2, and HAS3, have been identified and characterized (Rosa *et al*, 1988; Itano and Kimata, 1996a,b; Shyjan *et al*, 1996; Spicer *et al*, 1996; Watanabe and Yamaguchi, 1996; Spicer *et al*, 1997). The three HAS genes show distinct expression patterns (Spicer and Mcdonald, 1998) and the synthases are significantly different in their enzymatic properties and in their role in the pericellular hyaluronan coat formation (Itano *et al*, 1999). The precise regulatory mechanism of the expression of each HAS is still unknown. It has been shown that the synthesis of hyaluronan is stimulated by some growth regulatory factors and anti-inflammatory cytokines such as epidermal growth factor (EGF) and IL-1β (Heldin *et al*, 1989; Yung *et al*, 1996; Kaback and Smith, 1999), which have also been shown to be agents that promote wound healing (Brown *et al*, 1986; Gailit *et al*, 1994). Considering the above findings on the existence of three different hyaluronan synthases, it is likely that the expression of each hyaluronan synthase is regulated in a different manner, depending on the difference of growth regulatory factors or cytokines.

Langer and Vacanti (1993) described a new technology for solid organ transplants called *tissue engineering*, which involves the morphogenesis of new tissue using constructs formed from isolated cells cultured with growth regulatory factors and biocompatible scaffolds. Ueda *et al* (1995) fabricated cultured epithelium sheets for skin repair using cultured human oral mucosal epithelial (COME) cells and attained good clinical results. Therefore, we focused on the relationship among the growth regulatory factors, extracellular matrix, and epidermal and dermal cells, with the aim of tissue regeneration without scarring.

Most skin lesions heal rapidly and efficiently within a week or two; however, scars remain where the collagen matrix has been poorly reconstituted. Oral mucosa, on the other hand, rarely suffers from scarring in the process of

Abbreviations: COME cells, cultured human oral mucosal epithelial cells; EGF, epidermal growth factor; HA, hyaluronan; hHAS, human hyaluronan synthase; IL-1β, interleukin-1β; ORF, open reading frame; PCR, polymerase chain reaction; RT-PCR, reverse transcriptase-polymerase

wound healing (Tsai *et al*, 1995) and appears to be different from skin in this regard. We have developed a method to fabricate cultured epithelium for skin repair using COME cells, which are a potential new source of cells for cultured epithelial grafts without scarring (Ueda *et al*, 1995). Therefore, comparison of the regulation of hyaluronan synthesis in oral mucosa with that in skin may yield important insights into the wound-healing processes characteristic of oral mucosa lesions. Histological analysis of the hyaluronan distribution in skin showed that this molecule is localized not only in the dermis but also in the epidermis (Tammi *et al*, 1984). The ability of keratinocytes to synthesize hyaluronan has been reported in both cell cultures (Brown and Parkinson, 1983) and organ cultures (Tammi *et al*, 1989; Agren *et al*, 1995). Skin grafts have been shown to promote wound closure by releasing a variety of cytokines (Krejci *et al*, 1991; Martin, 1997). Therefore, it is likely that the expression of three different hyaluronan synthases in the skin may be regulated by these factors. Actually, Sugiyama *et al* (1998) found that TGF-β upregulates *HAS 1* and *HAS2* expression independently in cultured human skin fibroblasts. Although HAS1, 2, and 3 mRNAs have been detected in various tissues by northern blot analyses (Spicer and Mcdonald, 1998), comparative studies on the distributions of HAS1, 2, and 3 expression as well as on the effect of cytokines on their expression between oral mucosa and skin have not yet been performed.

Real-time RT-PCR analysis enables one to detect quantitatively certain mRNAs in RNA samples, although careful attention must be paid to establishing suitable PCR conditions and primers (Gibson *et al*, 1996; Heid *et al*, 1996). In this study, we took advantage of this new method and also developed culture systems to assess the expression of the HAS1, HAS2, and HAS3 genes and hyaluronan synthesis in COME cells, oral mucosal fibroblasts, and skin dermal fibroblasts, and compared them before and after simulation by IL-1β or EGF. The current results may help to clarify some of the mechanisms of the different responses in wound healing between oral mucosa and skin, and define potential targets for specific therapy directed at modulating hyaluronan synthesis in tissue engineering.

Results

Stimulation of expression of HAS genes by IL-1β or EGF in human mucosal COME cells Using real-time RT-PCR analysis, we measured the absolute amounts of the mRNAs of the three different hyaluronan synthases, HAS 1, HAS2, and HAS3, in the COME cells. Comparisons of the expression among different samples by normalizing each of the absolute amounts enabled us to elucidate how the addition of IL-1β or EGF affected the expression of the HAS 1, HAS2, and HAS3 genes. Treatment of COME cells with 0.1–100 ng per mL of IL-1β or EGF for 3 h resulted in a marked increase in both HAS1 and HAS2 mRNAs (Figs 1 and 2). Maximal levels of HAS1 and HAS2 expression were attained at 100 ng per mL IL-1β and 0.1 ng per mL EGF, respectively. Since EGF at this concentration (0.1 ng per mL) is used as one of the supplements for HuMedia-KG2 medium (commercially available), our finding indicates that this medium is suitable at least for hyaluronan synthesis by

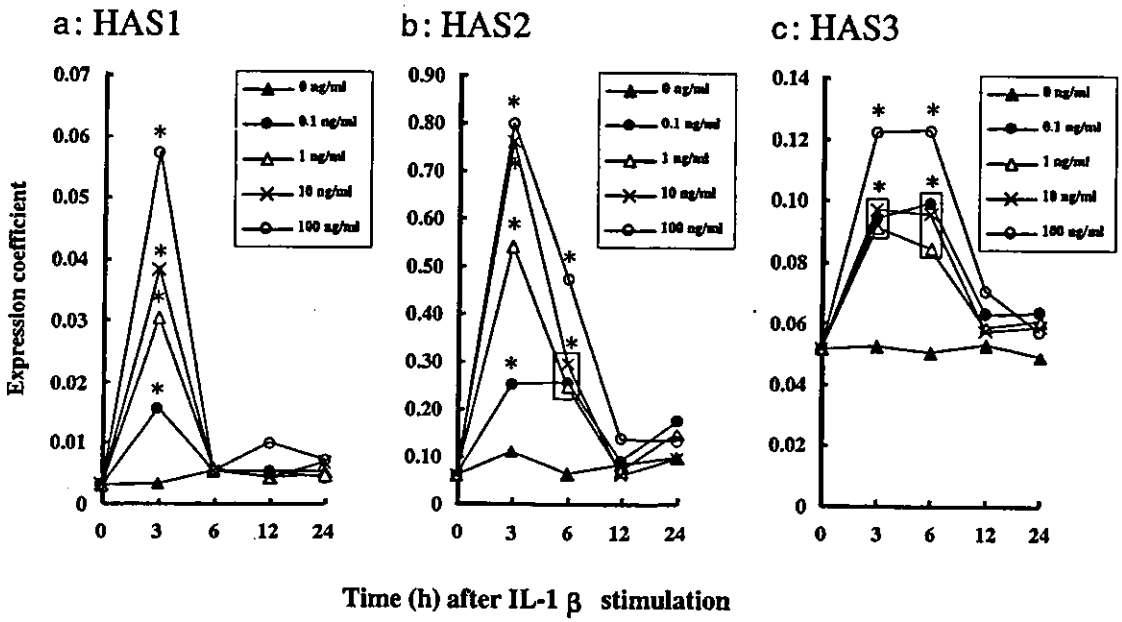

Figure 1
Stimulation by IL-1β of HAS1 (*a*), HAS2 (*b*), and HAS3 (c) gene expression in COME cells. COME cells were cultured in the presence of IL-1β at the indicated concentrations: 0 ng per mL (▲), 0.1 ng per mL (•), 1 ng per mL (△), 10 ng per mL (×), and 100 ng per mL (○). After 3, 6, 12, and 24 h, cells were lysed and total RNA were extracted. Total RNA were also extracted from the cells just before adding IL-1β as a control (0 h). Equal amounts of total RNA (200 ng) were subjected to real-time RT-PCR analysis, and the absolute amounts of mRNA of HAS1, HAS2, HAS3, and GAPDH in each sample were quantitated by comparison with their standard curves, as described in *Materials and Methods*. The expression coefficient for each mRNA (plotted on the ordinate) was calculated by dividing the absolute amount of each mRNA (HAS1, HAS2, and HAS3) by the absolute amount of GAPDH mRNA in each sample so that quantitative comparisons of the expression of each HAS mRNA could be made among the different samples. Each point is the mean value obtained from five independent experiments in which the differences were less than 10%. *Significantly different from the control value; $p < 0.01$. Boxed values are also significantly different ($p < 0.01$) from the control.

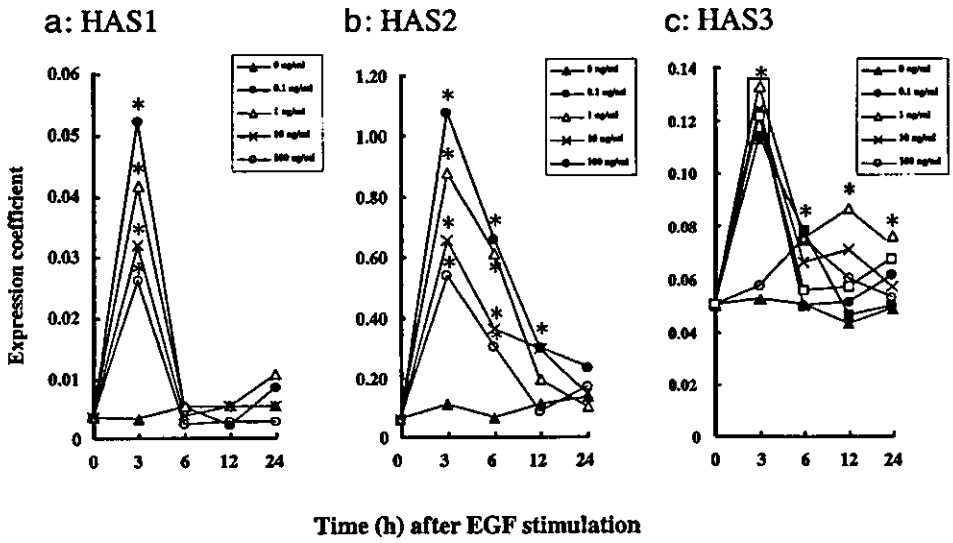

Figure 2
Stimulation by EGF of HAS1 (*a*), HAS2 (*b*), and HAS3 (*c*) gene expression in COME cells. COME cells were cultured in the presence of EGF at the indicated concentrations: 0 ng per mL (▲), 0.1 ng per mL (•), 1 ng per mL (△), 10 ng per mL (×), and 100 ng per mL (○). After 3, 6, 12, and 24 h, cells were lysed and total RNA were extracted. Total RNA were also extracted from the cells just before the addition of EGF as a control (0 h). The ordinate represents the expression coefficient for each mRNA, which was calculated as described in Fig 1. Each point is the mean value obtained from five independent experiments in which the differences were less than 10%. *Significantly different from the control value; $p<0.01$. Boxed values are also significantly different ($p<0.01$) from the control.

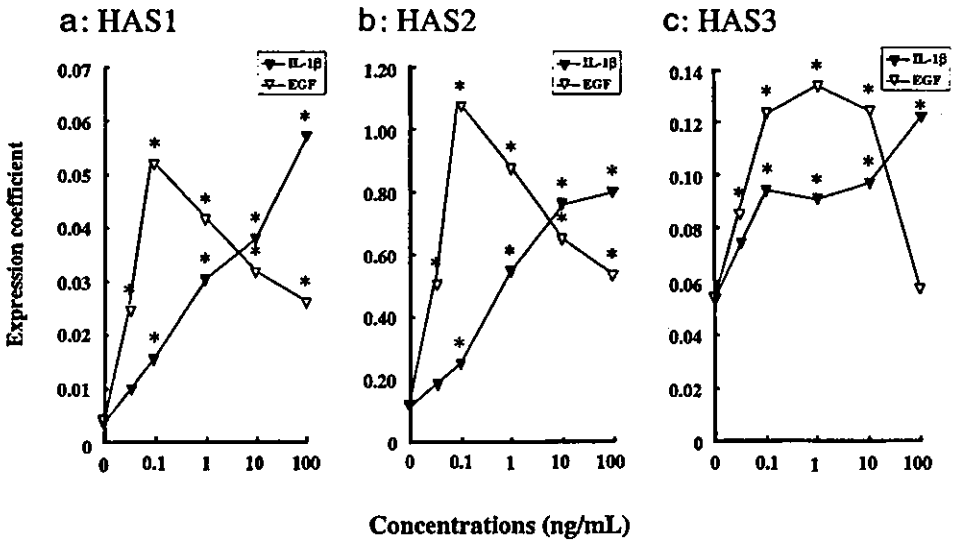

Figure 3
Comparison of concentration-dependent changes of HAS1 (*a*), HAS2 (*b*), and HAS3 (*c*) gene expression between stimulation by IL-1β or EGF. COME cells were cultured in the presence of the indicated concentrations of 0.1–100 ng per mL IL-1β (▼) or EGF (▽). After 3 h, cells were lysed and total RNA were extracted. Total RNA were also extracted from the cells just before the treatment for the 0 h sample. Quantitation of each mRNA (HAS1, HAS2, and HAS3) was performed using equal amounts of total RNA (200 ng) by real-time RT-PCR as described in *Materials and Methods*. The ordinate represents the expression coefficient for each mRNA, which was calculated as described in Fig 1. Each point is the mean value obtained from five independent experiments in which the differences were less than 10%. *Significantly different from the control value; $p<0.01$.

COME cells. The amounts of HAS1 and HAS2 mRNAs were increased in a concentration-dependent manner by IL-1β at all concentrations tested, while those in EGF-treated COME cells were maximal at 0.1 ng per mL EGF and decreased to almost the basal level at the higher concentrations of EGF in order of HAS1 and HAS expression (Fig 3). A much smaller increase of HAS3 than of HAS1 and HAS2 expression was observed in the early phase of the stimulation (Figs 1 and 2). The concentration-dependent changes in HAS3 expression after IL-1β or EGF stimulation were similar to, but less marked than, those in HAS1 and HAS2 expression (Fig 3).

Comparisons of expression coefficients at 3 h, when the maximal stimulation was observed, suggested that the absolute amount of HAS2 mRNA was about 20-fold that of HAS1 mRNA, and about 8-fold that of HAS3 mRNA in COME cells (Figs 1–3). Therefore, the HAS2 mRNA appeared to be responsible for most of the hyaluronan synthase expression in the early phase of IL-1β or EGF stimulation. The proportion of HAS3 mRNA, however, appeared to become more significant in the late phase of the stimulation (Figs 1 and 2).

Stimulation of HAS gene expression by IL-1β or EGF in cultured human oral mucosal and dermal fibroblasts We examined the effects of IL-1β or EGF on the expression of HAS1, HAS2, and HAS3 mRNAs in cultured oral mucosal fibroblasts and dermal fibroblasts using the same method. Stimulation of these fibroblasts with 0.1–100 ng per mL IL-1β or EGF for 3 h resulted in a marked increase of HAS1 mRNA in cultured dermal fibroblasts, HAS2 mRNA in both dermal and cultured oral mucosal fibroblasts, and HAS3 mRNA in cultured oral mucosal fibroblasts. Maximal levels of HAS1 and HAS2 expression were attained at 1 ng per mL IL-1β in dermal fibroblasts, while those of HAS2 and HAS3 expression were attained at 1 ng per mL EGF in oral mucosal fibroblasts (Fig 4). Neither significant HAS1 gene expression in cultured oral mucosal fibroblasts nor HAS3 gene expression in dermal fibroblasts was detected at any concentration of EGF or IL-1β (Fig 4). Interestingly, lower expression of the HAS2 gene was observed in both types of fibroblasts after EGF stimulation compared with that after IL-1β stimulation, whereas the opposite was observed in COME cells after EGF and IL-1β stimulation

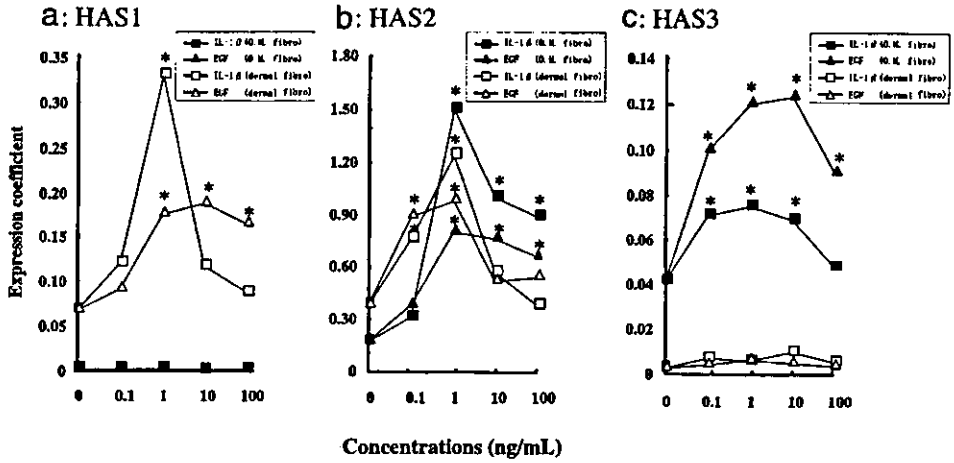

Figure 4
Comparison of concentration-dependent changes of HAS1 (*a*), HAS2 (*b*), and HAS3 (*c*) gene expression in oral mucosal and dermal fibroblasts between stimulation by IL-1β or EGF. Oral mucosal fibroblasts and dermal fibroblasts were cultured in the presence of the indicated concentrations of 0.1–100 ng per mL IL-1β (■ for oral mucosal fibroblasts, □ for dermal fibroblasts) or EGF (▲ for oral mucosal fibroblasts, △ for dermal fibroblasts) After 3 h, cells were lysed and total RNA were extracted. Total RNA were also extracted from the cells just before the treatment for the 0 h sample. Quantitation of each mRNA (HAS1, HAS2, and HAS3) was performed using equal amounts of total RNA (200 ng) by real-time RT-PCR as described in *Materials and Methods*. The ordinate represents the expression coefficient for each mRNA, which was calculated as described in Fig 1. Each point is the mean value obtained from five independent experiments in which the differences were less than 10%. *Significantly different from the control value; $p < 0.01$.

(compare concentration-dependency in Fig 4 with that in Fig 3).

We then investigated the upregulation of the expression of HAS1, HAS2, and HAS3 mRNAs when oral mucosal and dermal fibroblasts were stimulated with 1 ng per mL IL-1β or EGF for different periods. Treatment of oral mucosal fibroblasts with IL-1β or EGF resulted in marked and moderate increases, respectively, in the amount of HAS2 mRNA, with maximal stimulations at 6 and 3 h, respectively (Figs 5 and 6). On the other hand, the amount of HAS3 mRNA in mucosal fibroblasts was increased time dependently for at least 24 h by IL-1β stimulation, but reached a plateau with a 2-fold increase at 3 h in response to EGF stimulation (Figs 5 and 6). When dermal fibroblasts were treated with IL-1β or EGF, the upregulation of expression of HAS1 and HAS2 mRNAs was observed as early as 3 h after stimulation with either agent. The amount of HAS1 mRNA, however, was further increased time dependently up to 12 h, and then decreased to almost the basal level. The level of HAS2 mRNA was increased to a maximum at 6 h after IL-1β stimulation, decreased at 12 h, and again increased slightly thereafter. The maximal HAS2 expression level after IL-1β stimulation in dermal fibroblasts was 1.5 times higher than that after EGF stimulation (expression coefficient, 1.45 *vs* 0.93) (compare Fig 5 with Fig 6). The maximal stimulations by these cytokines of HAS1, HAS2, and HAS3 gene expression in both types of fibroblasts were mostly observed later than those in COME cells, as described above. The expression coefficients in Figs 5 and 6 suggest that in both types of cells, HAS2 mRNA was more abundant (about 5-fold) than the other HAS mRNAs.

These differences suggest that HAS1, HAS2, and HAS3 gene expression in oral mucosal and dermal fibroblasts is regulated by IL-1β and EGF in distinct manners that are cell-origin-specific and cytokine-specific.

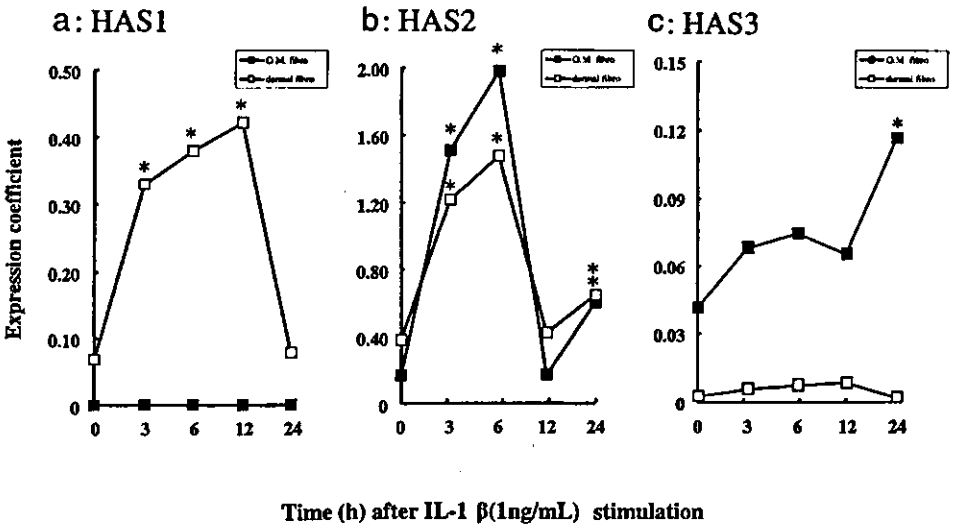

Figure 5
Comparison of stimulation by IL-1β of HAS1 (*a*), HAS2 (*b*), and HAS3 (*c*) gene expression between oral mucosal and dermal fibroblasts. Oral mucosal (■) and dermal (□) fibroblasts were cultured in the presence of 1 ng per mL IL-1β. After 3, 6, 12, and 24 h, cells were lysed and total RNA were extracted. For controls (0 h sample), total RNA were also extracted from the cells just before the addition of IL-1β. Quantitation of each mRNA (HAS1, HAS2, and HAS3) was performed using equal amounts of total RNA (200 ng) by real-time RT-PCR as described in *Materials and Methods*. The ordinate represents the expression coefficient for each mRNA, which was calculated as described in Fig 1. Each point is the mean value obtained from five independent experiments in which the differences were less than 10%. *Significantly different from the control value; $p < 0.01$.

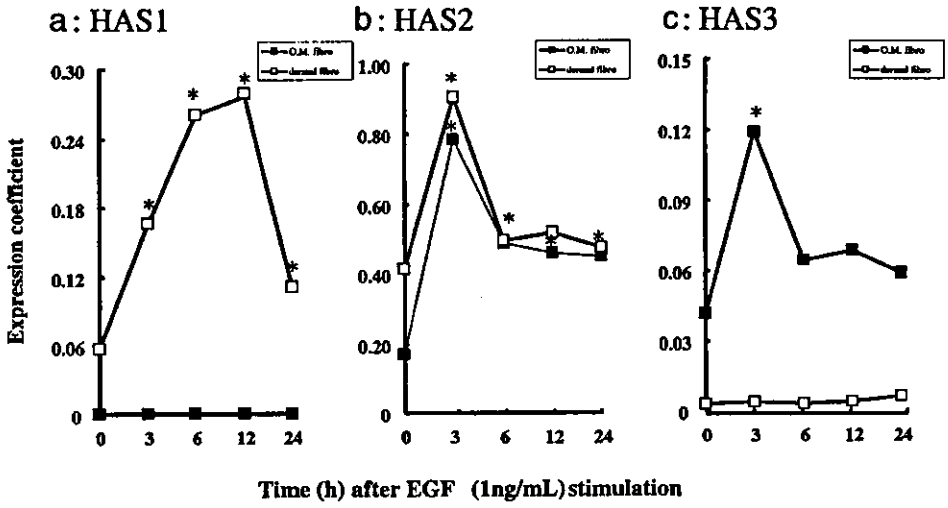

Figure 6
Comparison of stimulation by EGF of HAS1 (*a*), HAS2 (*b*), and HAS3 (*c*) gene expression between oral mucosal and dermal fibroblasts. Oral mucosal (■) and dermal (□) fibroblasts were cultured in the presence of 1 ng per mL EGF. After 3, 6, 12, and 24 h, cells were lysed and total RNA were extracted. For controls (0 h sample), total RNA were also extracted from the cells just before the addition of EGF. Quantitation of each mRNA (HAS1, HAS2, and HAS3) was performed using equal amounts of total RNA (200 ng) by real-time RT-PCR as described in *Materials and Methods*. The ordinate represents the expression coefficient for each mRNA, which was calculated as described in Fig 1. Each point is the mean value obtained from five independent experiments in which the differences were less than 10%. *Significantly different from the control value; $p < 0.01$.

Time course of IL-1β- or EGF-induced hyaluronan synthesis in cultured human COME cells, oral mucosal, and dermal fibroblasts To monitor the rate of hyaluronan synthesis at different times between 0 and 24 h after treatment with 1 ng per mL IL-1β or EGF, we measured the HA concentration in the culture medium at different times by a competitive ELISA-like assay, as shown in Fig 7. In COME cell cultures, IL-1β or EGF treatment induced an ~ 2–7-fold increase of newly synthesized hyaluronan during the stimulation, compared to the level at 3 h (Fig 7*a*). The amounts of HA in the cultures treated with either agent further increased time dependently up to 24 h. On the other hand, the amounts of HA in cultures of oral mucosal fibroblasts treated with IL-1β or EGF showed an ~ 23–47-fold increase, and that in cultures of dermal fibroblasts showed a 10–20-fold increase, compared to the levels at 3 and 6 h (Fig 7*b, c*). It is of note that neither oral mucosal fibroblasts nor dermal fibroblasts showed an IL-1β- or EGF-induced increase in hyaluronan synthesis until 6 h and that higher levels of HA were generated in oral fibroblasts than in dermal fibroblasts after IL-1β stimulation (Fig 7*b*), whereas higher levels of HA were observed in dermal fibroblasts than in oral mucosal fibroblasts after EGF stimulation (Fig 7*c*) Overall, it was interesting to see that the increased expression levels of HAS after IL-1β or EGF stimulation resulted in increased rates of HA synthesis, although concentration dependency of the increase of HA synthesis by these agents remains to be determined.

Discussion

A major goal of wound-healing biology is to discover how skin can be induced to reconstruct damaged parts more perfectly (Martin, 1997). In this regard, we firstly noted the previous observation that oral mucosa rarely suffers from

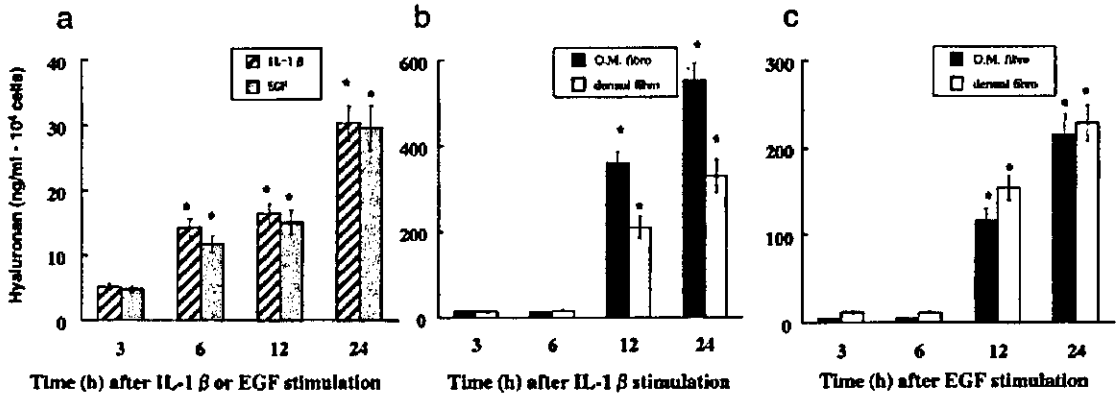

Figure 7
Time course of hyaluronan synthesis after the addition of IL-1β or EGF to COME cells (*a*), and after the stimulation of oral mucosal (■) and dermal fibroblasts (□) by IL-1β (*b*) or EGF (*c*). HA concentrations of the conditioned media of 3, 6, 12, and 24 h cultures were measured by a competitive ELISA-like assay as described in *Materials and Methods*. Each value was calculated by subtracting the control value from the sample value. The control HA activities were about 14.3 (ng per mL 10^4 cells) in COME cells (*a*), 93.6 (ng per mL 10^4 cells) in oral mucosal fibroblasts, 115 (ng per mL 10^4 cells) in dermal fibroblasts, and these values varied only slightly at different times (3, 6, 12, and 24 h). (*a*) COME cells were cultured in the presence of 1 ng per mL IL-1β or EGF (*b*) Oral mucosal and dermal fibroblasts were cultured in the presence of 1 ng per mL IL-1β. (*c*) Oral mucosal and dermal fibroblasts were cultured in the presence of 1 ng per mL EGF. Each column represents the mean ± SD of three separate experiments. *Significantly different from the value at 3 h; $p < 0.01$.

scarring in the process of wound healing and appears to be different from skin (Tsai *et al*, 1995), and therefore focused on differences in physiological responses to wound healing between oral mucosa cells and skin cells in this study. Wound healing involves many dynamic cellular processes, such as cell proliferation, cell migration, cell–cell interaction, and inflammation (Martin, 1997). It has been found that hyaluronan is deeply involved in these dynamic cellular processes during wound healing and inflammation (Knudson *et al*, 1989; Turley, 1989; Weigel *et al*, 1997). It is also known that some cell growth factors and cytokines facilitate wound healing and re-epithelialization by stimulating keratinocyte proliferation and migration (Clark and Henson, 1988; Gailit *et al*, 1994; Hubner *et al*, 1996; Martin, 1997; Tammi and Tammi, 1998; Pienimaki *et al*, 2001). Therefore, in this study we examined the relationships between hyaluronan synthesis and cellular responses to two cell growth regulatory factors involved in wound healing of the skin, namely IL-1β and EGF.

The present results demonstrated that the expression of the three different HAS genes was increased in COME cells by IL-1β or EGF treatment, and there was a corresponding increase of hyaluronan synthesis in these cells after the treatments. Therefore, such treatments may induce changes in the extracellular environment via the increased synthesis and accumulation of hyaluronan. The present data also showed that the stimulations varied with different concentrations and times of treatment with the cytokines and that the stimulation patterns were highly dependent upon cell origins. This may be important for understanding the difference in wound healing between oral mucosal epithelium and epidermis.

Our present study did not focus on human keratinocytes, because they have already been studied in detail in a few studies, with the following results. Sugiyama *et al* (1998) showed that human keratinocytes expressed HAS1 mRNA and a trace of HAS2 mRNA, and that when the culture was stimulated with TGF-β, HAS1 mRNA in keratinocytes was upregulated but HAS2 mRNA was not. A more recent study by Pienimaki *et al* (2001) showed that HAS2 mRNA was expressed in a rat keratinocyte cell line and EGF stimulation brought about an increase in HAS2 mRNA corresponding to about a 30-fold enhancement of hyaluronan production from the basal synthesis rate. They also showed that there was no increase in HAS1 or HAS3 in the cell line, but HAS2 mRNA increased 2–3-fold with less than 2 h following stimulation with EGF. Our present study on oral mucosal epithelium cells, however, demonstrated that in those cells the expression of HAS1 and HAS3 was upregulated after EGF stimulation, although these mRNAs were expressed at lower levels than HAS2 mRNA, and, in addition, HAS2 mRNA increased 2–11-fold depending on the concentration of the inducing agent (Fig 3). This finding may have depended on our use of the different cells or of the real-time RT-PCR method, which is more accurate than the methods used in earlier studies. Our finding also suggests that HAS1 and HAS3 might have distinctive effects on the wound healing of oral mucosal epithelia.

Sugiyama *et al* (1998) demonstrated that when human dermal fibroblasts were stimulated with TGF-β, both HAS1 and HAS2 mRNAs were upregulated. Zhang *et al* (2000) found by a quantitative study of HAS mRNA level that no HAS3 mRNA was detected in the RNA from human skin fibroblasts. We obtained similar results by quantitative real-time RT-PCR in our culture system of human dermal fibroblasts (Fig 4), although we used different cytokines. Our present study showed for the first time that HAS3 gene expression was detected in all of the mRNA samples obtained from human mucosal fibroblasts, but HAS1 gene expression was not detected. This unique HAS expression pattern of mucosal fibroblasts may be related to the unique feature of the lack of scarring in wound healing of oral mucosa epithelia.

It was interesting that the gradual increase in the amount of hyaluronan after the rapid and temporal increases in HAS mRNA expression after IL-1β or EGF treatment and the rates of hyaluronan synthesis differed, depending on the cell type and the stimulation agent (Fig 7). There have been several reports showing that the mRNA levels correlated with the levels of HAS proteins and with the production of hyaluronan (Jacobson *et al* (2000) for human mesothelial cells; Pienimaki *et al* (2001) for rat epidermal keratinocytes; Sayo *et al* (2002) for human keratinocytes). Pienimaki *et al* (2001) showed that the changes in HAS mRNA and hyaluronan synthesis levels showed a temporal correlation, suggesting tight transcriptional regulation of hyaluronan synthesis. In our study, however, in COME cells the hyaluronan synthetic rates increased gradually and time dependently with the maximal stimulation of the HAS mRNA expression at 3 h after IL-1β or EGF treatment, and the rate induced by IL-1β was higher than that induced by EGF. In both oral mucosal and dermal fibroblasts, the increased rates of hyaluronan synthesis were observed at later phases (12–24 h) than those of the mRNA expression. These differences suggest that the increased HAS enzyme proteins translated from the transiently increased amounts of the mRNAs resulting from the stimulation may have a long life span and produce hyaluronan continuously, especially in the cells stimulated by IL-1β. In addition, the turnover rates of the HAS mRNA may differ, depending on the cell type and way of stimulating the cells. In relation to the latter possibility, the gene structures, especially in the regulatory regions influencing the mRNA turnover, are different among the three HASs (Spicer and McDonald, 1998), and we previously characterized the promoter region of the mouse *HAS1* gene (Yamada *et al*, 1998). Investigation of the respective promoter sequences and identification of potential enhancer sequences for the three *HAS* genes and the respective stability of those HAS mRNAs will be necessary for understanding the differences in the responses of the genes to stimulation by various factors.

Jacobson *et al* (2000) pointed out that the cytokine inducibility of the transcripts of the three HAS genes might be widespread, but differ depending on the cell type. Heldin *et al* (1989) also showed that cytokines and growth factors regulate the rates of hyaluronan synthesis differently, depending on the cell type. Since there were differences in the experimental systems and conditions, exact comparisons between studies cannot be made. There are several examples, however, in previous reports suggesting that the above possibility is true. For example, Kaback *et al* (1999) showed substantial upregulation of hyaluronan synthesis in

orbital fibroblasts when they were activated with IL-1β. Hyaluronan synthesis in human synovial lining cells is stimulated by TGF-β and IL-1β, and to a lesser extent by TNF-α, and these cytokines have been suggested to be major factors leading to the development of joint swelling in inflammatory and degenerative joint diseases (Tammi and Tammi, 1998). In human keratinocytes, interferon-γ markedly upregulates HAS3 mRNA, whereas transforming growth factor β downregulates HAS3 transcript levels (Sayo *et al*, 2002). We found that in COME cells stimulated by IL-1β or EGF, there was a smaller increase of HAS3 expression compared to HAS1 and HAS2 expression at an early phase of the stimulation (Figs 1 and 2). Human peritoneal mesothelial cells also show a pronounced increase in hyaluronan synthesis upon IL-1β stimulation, and the resultant increase in the hyaluronan level in the peritoneal cavity was suggested to be relevant to the inflammation in peritonitis (Yung *et al*, 1996). In the mesothelial cells, the IL-1β stimulation caused a continuous time-dependent increase in hyaluronan synthesis, which appeared to be different from our present results demonstrating rapid and temporary stimulation of the expression of all of the HAS genes by IL-1β (Figs 1, 3, and 5). The effect of EGF on the hyaluronan synthesis in human foreskin fibroblasts did not show a sharp dependency on the EGF concentration (Heldin *et al*, 1989), but we found that the effect on HAS mRNA expression in oral mucosal fibroblasts and dermal fibroblasts did (Fig 4). Taken together, these facts imply that it is likely that different regulatory mechanisms for the expression of each of the three HAS genes and the stability of their transcripts control hyaluronan synthesis in different cells, which might lead to important differences in the physiological responses between oral mucosa cells and skin cells.

The general tendency for EGF to inhibit terminal differentiation and the ability of EGF to increase the synthesis of hyaluronan, which we observed in the present experiments, may be in accord with the previous results on the treatment of keratinocytes with hydrocortisone (Agren *et al*, 1995) and retinoic acid (Tammi *et al*, 1989), further strengthening the concept that enhanced hyaluronan synthesis is associated with the delayed cornification of keratinocytes and subsequent epidermal thickening (Clark and Henson, 1988; Tammi and Tammi, 1998). Therefore, regulating hyaluronan synthesis by using the cytokines EGF or IL-1β might be useful for adjusting the levels of hyaluronan in skin cells to levels equal to those in oral mucosal cells, and might thereby promote wound healing without scarring in the skin if this is applied to tissue engineering technology using living cells, cytokines, and growth factors.

Materials and Methods

Cell culture and RNA isolation Skin and oral mucosa (superfluous tissue obtained during surgery) were obtained from five patients treated in the Department of Oral Surgery and Plastic Surgery, Nagoya University Hospital. Donors gave informed consent. The cells were isolated by the method of Hata *et al* (1995). COME cells were routinely grown in HuMedia-KG2 medium (Kurabo, Osaka, Japan) (Boyce *et al*, 1983), supplemented with insulin (10 μg per mL), hydrocortisone (0.5 μg per mL), 4% (v/v) bovine pituitary extract, and EGF (0.1 ng per mL) plus various antibiotics.

To study the effects of IL-1β and EGF, COME cells were expanded by culturing in HuMedia-KG2 medium with the above supplements for 5 d. The cells were thoroughly washed with the medium without the supplements, dissociated by treatment with trypsin, and inoculated into plastic tissue culture dishes (35 mm) containing fresh medium at a density of 5.0×10^5 cells in the medium without EGF. At 48 h, the medium was exchanged and IL-1β or EGF (0.1–100 ng per mL) was added to the medium, and the cells were continuously cultured for the indicated times (0, 3, 6, 12, and 24 h). Total RNAs were extracted from the cells with an RNeasy Mini Kit (QIAGEN, GmbH, Hiden, Germany).

Human oral mucosal and dermal fibroblasts were grown in Dulbecco's modified Eagle's medium (DMEM) (Gibco Laboratories, Rockville, MD) containing 10% (v/v) fetal bovine serum and various antibiotics. In order to make the culture conditions identical to those used for studies on the stimulation of COME cells by IL-1β or EGF, the cells were grown for 14 d, dissociated with trypsin, and inoculated into plastic culture dishes (35 mm in diameter) at a density of 5.0×10^5 cells with HuMedia-KG2 medium as described above. At 48 h, the medium was refreshed and IL-1β or EGF was added to the medium at 0.1–100 ng per mL. The cells were then cultured for 0, 3, 6, 12, and 24 h and total RNAs were extracted as described above.

Preparation of absolute amounts of HAS1, HAS2, and HAS3 mRNAs Samples containing known amounts of HAS1, HAS2, and HAS3 RNAs were prepared for absolute comparison by real-time RT-PCR analysis. HAS1 cDNA was prepared as described previously (Itano and Kimata, 1996b). HAS2 and HAS3 cDNAs were obtained by PCR with the following pairs of primers—dGTGTTATACATGTCGAGTTTACTTCC (position 1475–1496 of the human *HAS2* ORF sequence) and dGTCATATTGTTGTCCCTTC-TTCCGC (position 1789–1766), and dGGTACCATCAGAAGTTCC-TAGGCAGC (position 83–108 of the human *HAS3* ORF sequence) and dGAGGAGAATGTTCCAGATGCG (position 411–391), respectively—and subcloned into pBluescript II KS vector (Promega, Madison, Wisconsin). The PCR amplification was carried out by 35 cycles of incubation, with each cycle consisting of denaturation at 94°C for 20 s, annealing at 58°C for 30 s, and extension at 68°C for 8 min. The PCR products were checked by electrophoresis on a 2% (w/v) agarose gel. The cDNAs were confirmed by sequencing these products. The DNAs containing the respective HAS cDNAs downstream of the T7 promoter were constructed and used as templates to synthesize RNAs *in vitro* by incubation with T7 RNA polymerase (Boehringer, Mannheim, Germany) according to the manufacturer's protocol. The RNAs were purified with an RNeasy Mini Kit (QIAGEN). The concentration of each RNA sample was determined by measuring the absorption (A_{260}) with a spectrophotometer.

Real-time RT-PCR analysis Real-time RT-PCR analysis was performed according to the reported method (Gibson *et al*, 1996; Heid *et al*, 1996). Briefly, within a gene-specific PCR oligonucleotide primer pair, an oligonucleotide probe labeled with a reporter fluorescent dye (FAM) at the 5′-end and a quencher fluorescent dye (TAMURA) at the 3′-end was designed. When the probe was intact, the reporter dye emission was quenched. During the extension phase of the PCR cycle, the nucleolytic activity of the DNA polymerase cleaved the hybridization probe and released the reporter dye from the probe. Fluorescence intensity produced during PCR amplifications was monitored by a sequence detector directly in the reaction tube ("real time"). A computer algorithm compared the amount of reporter dye emission with the quenching dye emission and calculated the threshold cycle number (C_T) when signals reached ten times the standard deviation of the baseline, from which the levels of the mRNAs transcribed from the various genes tested were obtained (Gibson *et al*, 1996).

Total RNA samples (200 ng of each) were added to a 50 μL RT-PCR reaction (PCR-Access, Promega). The "reaction master

Table I. Sequences of oligonucleotide primers and real time RT-PCR probes

Primer or Probe	Sequence	Position
hHAS1 900F	TGTGTATCCTGCATCAGCGGT	900–920
hHAS1 1072R	CTGGAGGTGTACTTGGTAGCATAACC	1072–1047
hHAS1 probeF	TAACCTCTTGCAGCAGTTTCTTGAGGCC	941–968
hHAS2 1475F	GTGTTATACATGTCGAGTTTACTTCC	1475–1496
hHAS2 1789R	GTCATATTGTTGTCCCTTCTTCCGC	1789–1766
hHAS2 probeF	TGGAACGTTGCTCTATGCATGCTATTGG	1692–1719
hHAS3 83F	GGTACCATCAGAAGTTCCTAGGCAGC	83–108
hHAS3 411R	GAGGAGAATGTTCCAGATGCG	411–391
hHAS3 probeF	TGGCTACCGAACTAAGTATACCGCGCGCTC	158–188

mixture" was prepared according to the manufacturer's protocol to give final concentrations of 1 × avian myeloblastosis virus Tfl reaction buffer, 0.2 mM dNTPs, 1.5 mM $MgSO_4$, 0.1 U per mL avian myeloblastosis virus reverse transcriptase, 0.1 U per μL Tfl DNA polymerase, 250 nM concentration of the primers, and 200 nM concentration of the corresponding probe, as described by Gibson *et al* (1996). Primers and probes for real-time PCR analysis of the hHAS1, hHAS2, and hHAS3 mRNAs were designed using the Oligo version 4.0 program (National Bioscience, Plymouth, Minnesota) according to Heid *et al* (1996). It has been shown that two or three transcripts that might be generated using alternative polyadenylation signals in the 3′-untranslated region exist for every HAS mRNA (Spicer and McDonald, 1998). In addition, there were differences in the 5′-terminal region sequence between the human HAS1 cDNAs cloned by us (Itano and Kimata, 1996b) and by Shyjan *et al* (1996). Therefore, this was taken into consideration when we designed the combinations of the primers. The sequences of all oligonucleotides used are shown in Table I. For the hHAS1 mRNA analysis, the primers hHAS1 900F and hHAS1 1072R were used and the probe was hHAS1TaqMan FP. For hHAS2 mRNA analysis, the primers hHAS2 1475F and hHAS2 1789R were used and the probe was hHAS2 TaqMan FP. For hHAS3 mRNA analysis, the primers hHAS3 83F and hHAS3 411R were used and the probe was hHAS3 TaqMan FP. The GAPDH primer and probe (TaqMan GAPDH detection reagents) were purchased from Perkin-Elmer and Applied Biosystems, Foster City, CA. RT-PCR reactions and the resulting relative increases in reporter fluorescent dye emissions were monitored in real time using a 7700 sequence detector (Perkin-Elmer). Signals were analyzed using the sequence detector 1.0 program (Perkin-Elmer). The conditions for PCR were as follows: an initial incubation at 50°C for 2 min, at 60°C for 30 min, and at 95°C for 5 min, followed by 50 cycles of incubation at 95°C for 20 s and 60°C for 1 min.

The absolute amount of each HAS mRNA in a given sample was obtained by comparison with the respective standard curves. Standard curves for each HAS mRNA were obtained using human heart t-RNA (Clontech, Palo Alto, California) with different concentrations (4000, 2000, 1000, 500, 250, 125, and 62.5 ng). Comparisons of the absolute amount of each mRNA for the three different HAS synthases among the different samples were made by using factors that were obtained by dividing the absolute amount of each mRNA by that of the GAPDH mRNA in each sample, and were designated as expression coefficients in this study.

Determination of HA concentrations by competitive ELISA-like assay Exponentially growing cells were cultured in fresh medium for 3, 6, 12, or 24 h, and the conditioned medium was recovered from each culture. The HA content of the conditioned medium was measured by a competitive ELISA-like assay as described previously (Itano *et al*, 1999). Briefly, the conditioned medium was mixed with biotinylated HA binding protein (b-HABP) and incubated at 4°C for 20 h. The mixture was added to the HA-coated wells of 96-well plates, followed by incubation for 6 h at room temperature. Alkaline phosphatase-conjugated streptavidin was used as the secondary probe, and the enzymatic activity was measured by using *p*-nitrophenyl phosphate as the substrate. HA contents were calculated by using a standard curve.

Statistical analysis The Dunnett test was used for comparisons between control and experimental groups (Dunnett, 1964).

We are grateful to Drs Yukio Sumi, Hirokazu Mizuno, and Yuko Ito in the Department of Oral and Maxillofacial Surgery, to Yoshihisa Miyata in the Department of Dermatology, Nagoya University Graduate School of Medicine, to Dr Takao Kondo and Chiaki Inoue in the Department of Biology, Faculty of Science, Nagoya University, and to Manami Nagano at PE Applied Biosystems Field Application/Technical Support, Japan for help and technical advice, and to Drs. Masahiko Zako, Hidekazu Takagi, and Mamoru Yoshida for discussions. This work was supported in part by a Grant-in-Aid for Scientific Research on Priority Areas from the Ministry of Education, Culture, Sports, Science and Technology (MEXT); by a Grant-in-Aid for Young Scientists (B) from the Japan Society for the Promotion of Science; by a Grant-in-Aid for Science Research (B) from MEXT; by a Grant-in-Aid for research at the Matrix Glycoconjugate group, Research Center for Infectious Disease, Aichi Medical University, from MEXT; and by a special research fund from Seikagaku Corp.

DOI: 10.1111/j.0022-202X.2004.22332.x

Manuscript received July 23, 2003; revised September 30, 2003; accepted for publication November 4, 2003

Address correspondence to: Assistant Professor Yoichi Yamada, Center for Genetic and Regenerative Medicine, Nagoya University School of Medicine, 65 Tsuruma-cho, Showa-ku, Nagoya 466-8550, Japan. Email: yyamada@tsuru.med.nagoya-u.ac.jp

References

Agren UM, Tammi M, Tammi R: Hydrocortisone regulation of hyaluronan metabolism in human skin organ culture. J Cell Physiol 164:240–248, 1995

Boyce ST, Ham RG: Calcium-regulated differentiation of normal human epidermal keratinocytes in chemically defined clonal culture and serum free serial culture. J Invest Dermatol 81:33–40, 1983

Brown KW, Parkinson: Glycoproteins and glycosaminoglycans of cultured normal human epidermal keratinocytes. J Cell Sci 61:325–338, 1983